The Escherichia coli MFS-type transporter genes yhjE, ydiM, and yfcJ are required to produce an active bo3 quinol oxidase

B.K. Hassani, Crysten Blaby-Haas, Andreia Verissimo, Fevzi Daldal

PLOS ONE

RESEARCH ARTICLE

The *Escherichia coli* MFS-type transporter genes *yhjE*, *ydiM*, *and yfcJ* are required to produce an active bo_3 quinol oxidase

Bahia Khalfaoui-Hassani[1,2]*, Crysten E. Blaby-Haas[3,4], Andreia Verissimo[2,5], Fevzi Daldal[2]*

1 Université de Pau et des Pays de l'Adour, E2S UPPA, IPREM, UMR CNRS, Pau, France, **2** Department of Biology, University of Pennsylvania, Philadelphia, PA, United States of America, **3** US Department of Energy Joint Genome Institute, Lawrence Berkeley National Laboratory, Berkeley, CA, United States of America, **4** Lawrence Berkeley National Laboratory, The Molecular Foundry, Berkeley, CA, United States of America, **5** bioMT-Institute for Biomolecular Targeting, Geisel School of Medicine at Dartmouth, Hanover, NH, United States of America

* b.khalfaoui-hassani@univ-pau.fr (BK-H); fdaldal@sas.upenn.edu (FD)

Citation: Khalfaoui-Hassani B, Blaby-Haas CE, Verissimo A, Daldal F (2023) The *Escherichia coli* MFS-type transporter genes *yhjE*, *ydiM*, *and yfcJ* are required to produce an active bo_3 quinol oxidase. PLoS ONE 18(10): e0293015. https://doi.org/10.1371/journal.pone.0293015

Editor: Tarunendu Mapder, Bristol-Myers Squibb Company, UNITED STATES

Received: July 24, 2023

Accepted: October 4, 2023

Published: October 20, 2023

Peer Review History: PLOS recognizes the benefits of transparency in the peer review process; therefore, we enable the publication of all of the content of peer review and author responses alongside final, published articles. The editorial history of this article is available here: https://doi.org/10.1371/journal.pone.0293015

Data Availability Statement: All relevant data are within the paper and its Supporting Information files.

Abstract

Heme-copper oxygen reductases are membrane-bound oligomeric complexes that are integral to prokaryotic and eukaryotic aerobic respiratory chains. Biogenesis of these enzymes is complex and requires coordinated assembly of the subunits and their cofactors. Some of the components are involved in the acquisition and integration of different heme and copper (Cu) cofactors into these terminal oxygen reductases. As such, MFS-type transporters of the CalT family (*e.g.*, CcoA) are required for Cu import and heme-Cu_B center biogenesis of the cbb_3-type cytochrome *c* oxidases (cbb_3-Cox). However, functionally homologous Cu transporters for similar heme-Cu containing bo_3-type quinol oxidases (bo_3-Qox) are unknown. Despite the occurrence of multiple MFS-type transporters, orthologs of CcoA are absent in bacteria like *Escherichia coli* that contain bo_3-Qox. In this work, we identified a subset of uncharacterized MFS transporters, based on the presence of putative metal-binding residues, as likely candidates for the missing Cu transporter. Using a genetic approach, we tested whether these transporters are involved in the biogenesis of *E. coli* bo_3-Qox. When respiratory growth is dependent on bo_3-Qox, because of deletion of the *bd*-type Qox enzymes, three candidate genes, *yhjE*, *ydiM*, and *yfcJ*, were found to be critical for *E. coli* growth. Radioactive metal uptake assays showed that Δ*ydiM* has a slower ^{64}Cu uptake, whereas Δ*yhjE* accumulates reduced ^{55}Fe in the cell, while no similar uptake defect is associated with Δ*ycfJ*. Phylogenomic analyses suggest plausible roles for the YhjE, YdiM, and YfcJ transporters, and overall findings illustrate the diverse roles that the MFS-type transporters play in cellular metal homeostasis and production of active heme-Cu oxygen reductases.

Funding: This work was supported by DOE grant DE-FG02-91ER20052 (FD). Work at the Molecular Foundry was supported by the Office of Science, Office of Basic Energy Sciences, of the U.S. Department of Energy under Contract No. DE-AC02-05CH11231 (CEB-H). Work at the U.S. Department of Energy Joint Genome Institute (https://ror.org/04xm1d337), a DOE Office of Science User Facility, is supported by the Office of Science of the U.S. Department of Energy operated under Contract No. DE-AC02-05CH11231 (CEB-H). The funders had no role in study design, data collection and analysis, decision to publish, or preparation of the manuscript.

Competing interests: The authors have declared that no competing interests exist.

Abbreviations: Cu, copper; cbb_3, Cox; cbb_3, type cytochrome *c* oxidase; bo_3, quinol oxidase; bo_3, Qox; HCO, heme-copper oxidases; TM, transmembrane; MFS, major facilitator superfamily; reverse transcription-PCR; RT-PCR, DDM, *n*-Dodecyl β-D-maltoside; UQ1, ubiquinol-1; Na_2S, sodium disulfide; KCN, potassium cyanide.

Introduction

Respiratory complexes are oligomeric membrane proteins with multiple cofactors, which are widely distributed among prokaryotes and eukaryotes. Their biogenesis is an intricate process involving the insertion of appropriate cofactors into the subunits and assembly of mature subunits into functional enzymes [1–3]. The cytochrome *c* oxidases (Cox) and quinol oxidases (Qox) catalyze the terminal steps of aerobic respiration, which is a four-electron reduction of oxygen to water [4–6]. Both enzymes are multi-heme complexes containing different types of hemes (*a*, *b*, and *c*) [4–6]. However, the two types of oxidases are different with respect to their electron donors as substrates. Cox employs extra-cytoplasmic water-soluble or membrane-attached *c*-type cytochromes, whereas Qox uses lipid-soluble membrane-integral quinones. The aa_3-type cytochrome *c* oxidase (aa_3-Cox or mitochondrial complex IV) contains two *a*-type (*a* and a_3) hemes and also two Cu centers (Cu_A with two Cu atoms and Cu_B with one Cu atom near of the Fe atom of heme a_3) [7–9]. The cbb_3-type cytochrome *c* oxidase (cbb_3-Cox) is exclusively found in prokaryotes, and it contains three *c*-type (c_o, c_{p1} and c_{p2}) hemes, two *b*-type (*b* and b_3) hemes and only one Cu atom near heme b_3 iron at the Cu_B center) [10–12]. Some Qox enzymes, like the *Escherichia coli* bo_3-type Qox (bo_3-Qox), also contain one Cu atom at their Cu_B center [13] like that of the aa_3-Cox or the cbb_3-Cox [14,15]. The nature of the cofactors, subunit structures, and electron donors vary among the heme-Cu oxygen reductases but their catalytic Fe-Cu_B centers remain conserved [15,16]. Besides bo_3-Qox, *E. coli* has two other *bd*-type Qox enzymes (*bd*-Qox1 and *bd*-Qox2) involved in aerobic respiration, but they contain no Cu atom [6,17,18].

Earlier studies indicated that covalent insertion of the *c*-type hemes to apoproteins is carried out by the cytochrome *c* maturation (*ccm*) systems (*e.g.*, cbb_3-Cox) [19]. The Ccm systems operate independently from the insertion of axially coordinated *a*-, *o*-, and *b*-type hemes [2,12]. Coordination of the *b*-type hemes to the apoproteins may be spontaneous, like the soluble four-helical cytochrome b_{562} [20]. In other cases, the process might be chaperone-assisted, like the *a*-type hemes of aa_3-Cox that rely on the Surf-like (Surf1 or Shy1) proteins [21–24]. In *Paraccocus denitrificans* Surf1 [23] and in *Thermus thermophilus* Surf1q and CbaX [25] are essential to produce active ba_3-type quinol oxidases (ba_3-Qox), possibly needed for the insertion of the *a*-type hemes. Similarly, the insertion of the *b*-type hemes to the facultative photosynthetic model organism *Rhodobacter capsulatus* cbb_3-Cox requires the CcoS protein [26,27]. While the small protein CydX was proposed to position/stabilize the *b*-type hemes of the *bd*-type quinol oxidase [18,28,29], this process remains unknown in bo_3-Qox.

In contrast to the heme groups, Cu insertion into the Cox enzymes has been studied in more detail. In *Rhodobacter* species, the mitochondrial Sco-like proteins [30] SenC or PrrC [31–34], PCuAC-like (PccA) [32,33,35], and Cox11 [36–39] chaperones are involved in this process [39–42]. In the case of cbb_3-Cox, Cu is imported by a MFS-type transporter (CcoA) and reduced via a cupric reductase (CcoG) on its way to the cytoplasm [2,43]. Then, Cu is channeled through a specific chaperone (CopZ) and a P_{1B}-type transporter (CcoI, CtpA or CopA2) to the periplasmic Sco-like and PCuAC-like chaperones [2,26,44,45], in its way to the Cu_B center of cbb_3-Cox [2,46–48]. In *R. capsulatus*, *ccoA* mutants are cbb_3-Cox Cu-deficient and unable to import radioactive ^{64}Cu [46,47]. This cytoplasmic deficiency can be rescued either by exogenous Cu supplementation, or by deletion of the P_{1B}-type Cu exporter CopA, involved in excretion of excess Cu out of the cytoplasm. Remarkably, similar studies in *Rhodobacter sphaeroides* indicated that CcoA is solely dedicated to Cu insertion into the cbb_3-Cox and is not required for the similar heme-Cu_B center of aa_3-Cox [49]. For the eukaryotic aa_3-Cox, Cu located in the mitochondrial intermembrane space is conveyed to the Cu_A center via Cox17 [40–42]. Although no homologue of Cox17 exists in prokaryotes, recently, the

Bradyrhizobium japonicum ScoI homologue and the thioredoxin TlpA were shown to metalate *in vitro* the Cu_A center of cognate aa_3-Cox [50,51]. Apparently, distinct Cu routes for the biogenesis of similar centers occur in species containing different types of Cox enzymes.

The superfamily of MFS-type transporters belongs to one of the largest groups of secondary active transporters and are exceptionally diverse and ubiquitous to all three kingdoms of living organisms. They selectively transport a wide range of substrates, including sugars, amino acids, peptides, and antibiotics [52]. Despite their structural similarities, members of this superfamily are divided into many families and subfamilies, classified in the IUBMB-approved Transport Classification Database (TCDB, http://www.tcdb.org), based on the diversity of their substrates and their modes of transport (uniporters, symporters, and antiporters). To date, about 105 families of the MFS-type transporters are reported [53], and among them about 28 are classified as Uncharacterized Major Facilitators (UMFs). The CalT subfamily is defined based on their conserved MXXXM and HXXXM motifs [49] and phylogenetic relatedness. They also frequently co-occur with the Cox enzymes [48,49]. The *R. capsulatus* CcoA is the founding member of this subfamily as the first bacterial Cu uptake transporter involved in the biogenesis of the cbb_3-Cox [46], and is also the first MFS-type transporter that uses Cu as a substrate [48,49]. Some CcoA-distant members (*i.e.*, the RfnT-like proteins) of the CalT family are also Cu transporters but they do not provide Cu to the cbb_3-Cox [48], suggesting that they might play a role in the biogenesis of other cupro-enzymes.

In this work, the role of MFS-type transporters of unknown function (UMFs) in *E. coli* bo_3-Qox biogenesis was investigated employing a genetic approach. Using mutants lacking both the *bd*-Qox1 and *bd*-Qox2 enzymes, where the bo_3-Qox was the only intact terminal oxidase, the uncharacterized MFS-type transporters YhjE, YdiM, and YfcJ were shown to be required to produce active bo_3-Qox to support *E. coli* aerobic respiration. Of these UMFs, YhiE and YdiM affected cellular Fe and Cu homeostasis, respectively, suggesting that MFS-type transporters are required for the biogenesis of different heme-Cu oxygen reductases, possibly as metal or related compound transporters.

Materials and methods

Growth conditions, strains and plasmids used

The bacterial strains and plasmids used in this work are described in **S1 Table in S1 File**. All *E. coli* K-12 strains were grown at 37˚C on Luria Bertani (LB) enriched or M9 minimal media, supplemented with ampicillin (Amp, 100 μg/ml) and kanamycin (Km, 50 μg/ml), as appropriate. For anaerobic growth, liquid cultures in filled vessels and plates placed in anaerobic jars with H_2+CO_2 generating gas-packs (Becton, Dickinson and Co., MD) were used. The optical density (OD_{600}) of cells in liquid cultures were monitored at 600 nm.

Kan^S derivatives of the MFS-type transporter mutants

The putative MFS-type transporter mutants Δ*setC*, Δ*yhjE*, Δ*yhjX*, Δ*ynfM*, Δ*ydiM*, Δ*yebQ*, Δ*yfcJ*, Δ*araJ* and the Δ*cyoB* mutant were obtained from the *E. coli* Keio library and were Kan^R [54]. In each case, the kanamycin cassette was removed by introduction of the Flp recombinase carried by the plasmid pEL8 (pCP20) [55], which is Amp^R and temperature sensitive (Ts) for replication. After electroporation, Amp^R mutants harboring pEL8 were grown at 30˚ C on LB containing ampicillin to allow excision of the *kan* cassette via its FRT sites located adjacent to it. Plates were transferred to 42˚ C to eliminate the Amp^R provided by pEL18, and the genotypes of the Kan^S and Amp^S colonies were confirmed by PCR using appropriate primers (**S2 Table in S1 File**).

Construction of the Δbd-Qox1and Δbd-Qox1+Δbd-Qox2 knockout derivatives of selected MFS-type transporter mutants

The Kan^S and Amp^S derivatives of chosen MFS-type transporter mutants were used as recipients to knockout the *bd*-Qox1 and *bd*-Qox2 by P1 transduction. The *Δbd*-Qox1 derivatives of the MFS-type transporter mutants were obtained by using a P1 lysate grown on fresh cultures of the *cydB*:*kan* (Δ*bd*-Qox1) strain, in LB medium supplemented with 0.2% glucose and 5 mM $CaCl_2$. Before use, the P1 lysates were sterilized with a few drops of chloroform, and the recipient cells were mixed with the P1(*cydB*::*kan*) lysate (at 1:1 v/v ratio), incubated 20 min at 37˚C, supplemented with one volume of 1M $CaCl_2$ and further incubated for 40 min at 37˚C in LB medium. The Kan^R (*i.e.*, Δ*bd*-Qox1) transductants were selected on kanamycin containing plates supplemented with 5 mM sodium citrate to chelate Ca^{++} required for P1 reinfection. Following extensive purification, the genotypes of the double (*i.e.*, ΔMFS + Δ*bd*-Qox1) mutants were confirmed by PCR using the primers listed in **S2 Table in** S1 File.

To construct the triple (*i.e.*, ΔMFS + Δ*bd*-Qox1 + Δ*bd*-Qox2) mutants, the Kan^R marker in the *cydB* gene of the ΔMFS + Δ*bd*-Qox1 double mutants was removed using pEL8 as described above. The Kan^S derivatives thus obtained were used to knock out the *bd*-Qox2 by transduction using a P1 lysate obtained by growth on the Δ*appB*::*kan* (*bd*-Qox2) mutant. The triple mutants lacking both the *Δbd*-Qox1, *Δbd*-Qox2 and the desired deletion of MFS-type transporter were selected on kanamycin containing plates, and their genotypes confirmed by PCR using the primers listed in **S2 Table in** S1 File.

RNA isolation and RT-PCR assays

The *E. coli* cells used for RNA isolation and subsequent RT-PCR analyses were grown aerobically at OD_{600} of 0.05, 0.1 (early growth) and 0.15 (late growth), as needed. Prior to RNA extraction, the cultures were washed with sterile water treated with two volumes of "RNAprotect Bacteria Reagent" (Qiagen). The total RNA was extracted using the Qiagen RNeasy mini kit according to the "Enzymatic Lysis of Bacteria" protocol of the manufacturer. 10 μg of total RNA was digested with RNAse-free Dnase I from Qiagen for 25 min at room temperature, followed by overnight precipitation using 20 μl of NaOAc (3M, pH 5.5), 3 μl of glycogen (5mg/ml), and 600 μl ethanol in a final volume of 800 μl. 2 ng of total RNA were used for RT-PCR analyses with OneStep RT-PCR kit from Qiagen using the CyoAQ-F/CyoAQ-R (327 bp amplicon), CyoBQ-F2/CyoBQ-R3 (322 bp amplicon), CyoCQ-F/CyoCQ-R (344 bp amplicon), and CyoDQ-F/CyoDQ-R (310 bp amplicon) primer pairs (**S2 Table in** S1 File) to reverse transcribe and amplify separately portions of mRNA specific of *cyoA*, *cyoB*, *cyoC*, and *cyoD*, respectively. The RrsA-F1 and RrsA-R1 primers were used as an internal control to reverse transcribe and amplify a 100 bp long portion of the 16S ribosomal mRNA. DNA contamination was checked using the master mix containing the heat-inactivated reverse transcriptase (95˚ C, 15 min) prior to the RT-PCR analyses. The amplified products were separated using 2% agarose gel, and their intensities estimated using ImageJ software (NIH).

Reduced-minus-oxidized optical difference spectra

To monitor the presence of bo_3-Qox in appropriate *E. coli* mutants, optical spectra of *n*-dodecyl β-D-maltoside (DDM)-solubilized membranes from cells grown aerobically at OD_{600} of 0.1 were recorded at room temperature between the 500 and 600 nm using a Varian Cary 50 UV-visible spectrophotometer. DDM-solubilized membrane fractions (final concentration of 5 mg/mL) were prepared in 25 mM Tris-HCl pH 7.0, 150 mM NaCl and 1 mM 4-benzenesulfonyl fluoride hydrochloride (AEBSF). Reduced *minus* oxidized optical difference spectra were

obtained by subtracting the spectra of samples fully reduced with sodium dithionite from the spectra of samples fully oxidized with potassium ferricyanide to detect the bo_3-Qox.

Determination of the bo_3-Qox enzyme activity

The oxygen consumption activity of bo_3-Qox was monitored using a Clark-type oxygen electrode (INSTECH, Sys203 model). The cells were grown on LB medium to an OD_{600} of 0.1, washed with 0.1 M potassium phosphate buffer, pH 7.0 and resuspended in the same buffer to a total of OD_{600} of 0.5 per assay. 400 μM of ubiquinol-1 was used as an artificial electron donor in the presence of 5 mM of DTT, and the electrode chamber contained one ml of the assay buffer (0.1 M potassium phosphate, pH 7.0, and 0.05% of DDM) at 30˚C. The enzymatic reaction was initiated by adding the cells. When tested for inhibitor sensitivity, cells were incubated with either 10 μM of sodium sulfide (Na_2S) or 200 μM of potassium cyanide (KCN) for 2 min prior to addition to the reaction mixture. The μM of oxygen consumed/min/OD_{600} of cells were calculated using the formula: Δmm-Hg x 236/140/min/OD_{600} of cells (140 mm-Hg corresponding to 236 μM of oxygen at 30˚ C was taken as the maximum of oxygen present in the electrode chamber).

Radioactive ^{64}Cu and ^{55}Fe uptake assays using whole cells

Whole cells radioactive ^{64}Cu uptake assays were performed according to [47]. The radioactive ^{64}Cu (1.84 x 10^4 mCi/μmol specific activity) was obtained from the Mallinckrodt Institute of Radiology, Washington University Medical School. *E. coli* strains were grown at an OD_{600} of 0.1 in 10 ml of LB supplemented with the appropriate antibiotics, centrifuged, washed with the assay buffer (50 mM sodium citrate, pH 6.5 and 5% glucose) and re-suspended in one ml of the same buffer. All cultures were normalized to the same number of total cells (7.5 X 10^8 cells) per 500 μl based on their OD_{600} values. Cells were pre-incubated at 35˚ C or 0˚ C for 10 min before the assay, and the uptake activity was initiated by addition of 10^7 cpm of ^{64}Cu, determined immediately before use (half-life of ^{64}Cu isotope is ~ 12 h). At each time point, 50 μl of 1 mM $CuCl_2$ and 50 μl of 50 mM EDTA (pH 6.5) were added to an aliquot of 50 μl of assay mixture to stop the uptake reaction, and the samples were placed on ice. At the end of the assay, cells were pelleted, pellets washed twice with 100 μl of ice-cold 50 mM EDTA solution, re-suspended in 1 ml of scintillation liquid, and counted using a scintillation counter (Coulter-Beckman Inc.) with wide open window. The uptake assay with ^{55}Fe (1 μmol correspond to 73 mCi/mg specific activity) was performed essentially as described for ^{64}Cu, except that 1M sodium ascorbate was added to the ^{55}Fe stock solution and incubated for 10 min at room temperature to reduce it prior to the assays. The assays were stopped using 1 mM of $FeSO_4$ instead of $CuCl_2$ and processed as described for the ^{64}Cu uptake assays.

Sequence comparison analyses

The protein sequence similarity networks were constructed using the EFI-EST tool (https://efi.igb.illinois.edu/efi-est/) [56] with an alignment score of 70 (YdiM), 110 (YhjE) or 80 (YfcJ), and nodes were collapsed at a sequence identity of 95% (ydiM) or 100% (YhjE and YfcJ). The networks were visualized with Cytoscape (https://www.cytoscape.org) [57] using the Prefuse Force Directed OpenCL Layout. For phylogenetic analyses, protein sequences were aligned using the CIPRES web portal [58] with MAFFT on XSEDE (v. 7.490) [59], and the IQ-TREE web server for construction of phylogenetic trees under maximum likelihood [60]. Trees were visualized with iTOL [61], and branches with less than 50% bootstrap support were deleted. Gene neighborhoods (a window of 10 genes upstream and downstream of the *ydiM*, *yhjE*, or

yfcJ homologues) were retrieved using the EFI-GNT tool (https://efi.igb.illinois.edu/efi-gnt/) [56]. The lists of proteins used for bioinformatic analyses can be found in **S1 Dataset**.

Statistical analyses

In all cases, at least three independent experiments were performed with at least three technical replicates. The error bars reflect the standard deviation with n indicating the number of independent repeats for each experiment. Statistical analyses were performed using the Student t-test with the wild-type activity as reference, and all p-values (when a phenotype is involved) were <0.05 as needed.

Results

Search for distant CcoA homologues among the E. coli MFS-type transporters

Homology searches were performed to identify putative CalT family members in *E. coli* that contains bo_3-Qox, but lacks cbb_3-Cox, to inquire whether the two similar heme-Cu_B center containing enzymes share analogous Cu-uptake pathways. Although CalT homologues are readily identified in species belonging to the Gammaproteobacteria [48,49], including *Pseudomonas aeruginosa*, *Shewanella pealeana*, and *Vibrio* species, none are found in the *Enterobacteriaceae*, including *E. coli* (EcoCyc, https://ecocyc.org). Currently there are about 70 ORFs annotated as an "MFS-type transporter" in the genomes of various *E. coli* strains, and about 28 of them have an unknown function (*i.e.*, UMFs). None of these UMFs contains the conserved hallmark (membrane-integral Cu-binding motifs MXXXM and HXXXM) of the CalT family members [11]. This observation suggested that cytoplasmic import of Cu inserted to the *E. coli* bo_3-Qox Cu_B center might be delivered by a CalT-unrelated transporter(s), like the *R. sphaeroides* aa_3-Cox [49]. However, this suggestion did not exclude whether any one of the UMFs could be involved in bo_3-Qox production. Consequently, these UMFs were scrutinized by aligning their amino acid sequences with that of the canonical CalT member (*i.e.*, *R. capsulatus* CcoA) and the occurrence of potential metal binding amino acid residues, like Cys, Met and His [62] (*Supplementary Materials*, **S1 Fig**). This search yielded eight candidates, *yfcJ*, *yhjX*, *yebQ*, *ynfM*, *ydiM*, *yhjE*, *araJ*, and *setC* that were studied further.

MFS-type transporters that affect the bo_3-Qox supported respiration in E. coli

E. coli contains three distinct terminal respiratory oxidases, the bo_3-Qox, *bd*-Qox-1 and *bd*-Qox-2 that convert oxygen to water during respiration. The bo_3-*Qox* is the major enzyme when oxygen concentration is high in the growth media, whereas *bd*-Qox-1 becomes predominant when the oxygen level is low [63,64]. Simultaneous absence of these enzymes renders *E. coli* defective for respiration. However, under certain conditions such as carbon and phosphate starvation, a third O_2 reductase, the *bd*-Qox-2 encoded by *appBCX*, could be induced [65,66]. The occurrence of suppressor mutations that turn on the *bd*-Qox-2 is frequent, and this event readily overcomes the respiratory defect of a double mutant lacking both bo_3-Cox and *bd*-Qox-1 [67]. Hence, assessing the role, if any, of the UMFs in the production of an active bo_3-Cox requires an *E. coli* strain lacking both the *bd*-Qox-1 and *bd*-Qox-2 enzymes. Such a double mutant renders the aerobic respiratory growth of *E. coli* exclusively dependent on the activity of bo_3-*Qox*. Thus, the double deletion Δ*bd-Qox1* + Δ*bd-Qox2* strain (strain BF24 with an active bo_3-Qox) and the triple Δbo_3-*Qox* + Δ*bd-Qox1* + Δ*bd-Qox2* mutant (strain BF17 with an inactive bo_3-Qox) were constructed as positive and negative controls for bo_3-Qox activity,

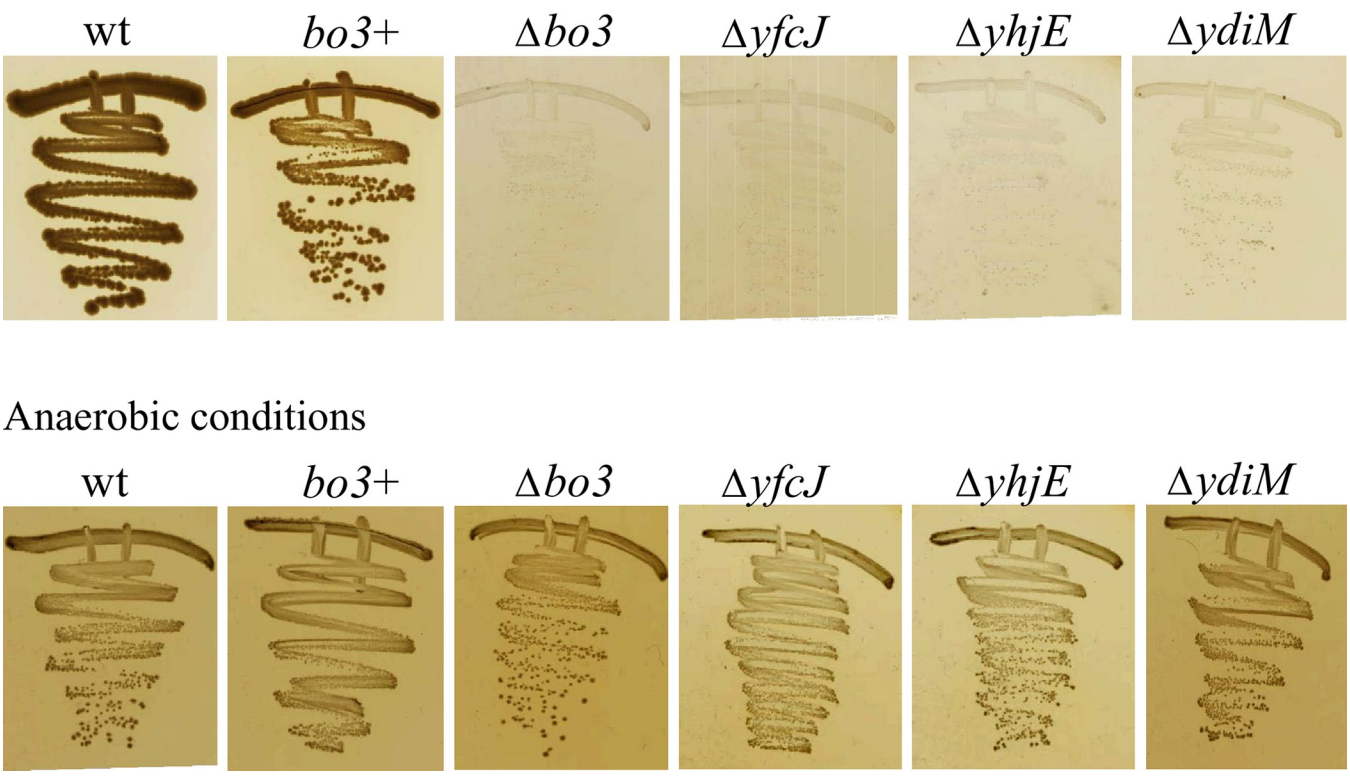

Fig 1. Growth phenotype of Δ*yfcJ*, Δ*yhjE*, and Δ*ydiM* mutants. The strains were grown on plates under either aerobic (top row) or anaerobic (bottow row) conditions. The parental strain is the *E. coli* K-12 (BW25113) used to generate the Keo library (**Materials** and **Methods**). In the bo_3^+ strain bo_3-Qox is the only functional quinol oxidase, whereas all quinol oxidases are absent in Δbo_3 strain, which does not grow under aerobic conditions. The MFS-type transporters mutants Δ*yfcJ*, Δ*yhjE*, and Δ*ydiM* lack *bd-Qox1* and *bd-Qox2* quinol oxidases, and unlike the bo_3^+ strain show poor aerobic growth phenotype like the Δbo_3 mutant bo_3-Qox.

https://doi.org/10.1371/journal.pone.0293015.g001

respectively, using the *E. coli* K-12 Keio collection library [54] (**Materials** and **Methods**). The deletion alleles of the desired UMFs, equally originating from the Keio library, were introduced under anaerobic growth conditions on minimal medium into the double deletion Δ*bd-Qox1* + Δ*bd-Qox2* background, and their aerobic respiratory growth phenotypes were determined in both minimal (M9) and enriched (LB) media. For the sake of simplicity, these mutants are referred to as bo_3^+ (double mutant Δ*bd-Qox1* + Δ*bd-Qox2* with active bo_3-Qox), Δbo_3 (triple mutant Δbo_3-*Qox* + Δ*bd-Qox1* + Δ*bd-Qox2* with inactive bo_3-Qox), and Δ*mfs* (triple mutant with a chosen Δ*mfs* + Δ*bd-Qox1* + Δ*bd-Qox2*, where Δ*mfs* corresponds to Δ*yfcJ*, Δ*yhjX*, Δ*yebQ*, Δ*nfM*, Δ*ydiM*, Δ*yhjE*, Δ*araJ*, or Δ*setC*, as appropriate).

As expected, the bo_3^+ (Δ*bd*-Qox1 and Δ*bd*-Qox2) strain grew aerobically, though less vigorously than the wild-type parental *E. coli* K-12 (BW25113) strain (**S1 Table in S1 File**), whereas the Δbo_3 strain showed no appreciable respiratory growth (**Fig 1**, top row). When respiratory growth was dependent solely on bo_3-Qox, the MFS-type transporter mutants Δ*setC*, Δ*yhjX*, Δ*ynfM*, Δ*yebQ*, and Δ*araJ* were respiration proficient like the bo_3^+ (Δ*bd*-Qox1 and Δ*bd*-Qox2) strain. In contrast, the Δ*yhjE* (BF22), Δ*ydiM* (BF23) and Δ*yfcJ* (BF21) mutants exhibited aerobic growth defect like the Δbo_3 strain while their anaerobic growth were fine (**Fig 1**, top and bottom rows). On aerobic-enriched medium, unlike the remaining Δ*mfs* derivatives or the bo_3^+ (Δ*bd*-Qox1 and Δ*bd*-Qox2) strain that can attain an OD_{600} of ~ 4 (with 1 h doubling time), the Δ*yhjE*, Δ*ydiM*, and Δ*yfcJ* mutants and the Δbo_3 strain can reach a maximum OD_{600}

of only ~ 0.15 (with ~ 4 h doubling time), indicating that their biomass yields were very low. The growth defect of the Δ*yhjE*, Δ*ydiM* and Δ*yfcJ* mutants in the absence of *bd*-Qox1 and *bd*-Qox2 suggested that these UMFs might be required to produce an active bo_3-Qox under aerobic growth conditions.

Effects of YhjE, YdiM, and YfcJ on the transcription of bo_3-Qox

Whether the aerobic growth defect seen in the Δ*yhjE*, Δ*ydiM* and Δ*yfcJ* mutants reflected the lack of transcription of the *cyoABCD* operon encoding the bo_3-Qox subunits was tested. As the aerobic growth is needed to produce the bo_3-Qox, transcription of *cyoB* gene by RT-PCR was used as a proxy for the *cyoABCDE* operon. Mutant cells grown under aerobic conditions at an OD_{600} of ~ 0.05 and ~ 0.1 (early stage of growth) showed that the *cyoB* transcript was detectable in the Δ*yhjE*, Δ*ydiM*, and Δ*yfcJ* mutants (Fig 2A). However, at later growth stages (OD_{600} of ~ 0.15 or above) where cell growth was arrested, the amounts of *cyoB* mRNA greatly decreased, possibly reflecting compromised mRNA transcription or stability upon growth stagnation (Fig 2B). Hence, the data indicated that at least at the early stage of growth the absence of *yhjE*, *ydiM* or *yfcJ* did not abolish the transcription of *cyoB*. Similar data were also obtained for the *cyoA*, *cyoC* and *cyoD* genes (S2 Fig, left lanes). Note that when these mutants were complemented with the multicopy plasmid pJRHisA overexpressing a wild type bo_3-Qox, the *cyoA*, *cyoB*, *cyoC* and *cyoD* transcripts were detectable at all growth stages (**S2 Fig,** right lanes).

Absence of YhjE or YdiM or YfcJ affects the enzymatic activity of bo_3-Qox

The bo_3-Qox activities of the Δ*yhjE*, Δ*ydiM* and Δ*yfcJ* mutants (in the Δ*bd-Qox1* Δ*bd-Qox2* background) were monitored using whole cells at their early stage of growth (at OD_{600} = 0.1, *i.e.*, *cyoABCDE* transcript is like the parent), using a Clark-type oxygen electrode and ubiquinol-1 (UQ1) as an electron donor (Materials and Methods). Under these conditions, the bo_3^+ (Δ*bd*-Qox1 and Δ*bd*-Qox2) strain exhibited ~ 34 μmoles of O_2 consumed/min/OD_{600} of cells (referred to as 100%). This activity was inhibited by the addition of 10 μM of the bo_3-Qox specific inhibitor Na_2S (to ~ 15%) or 200 μM of Cox or Qox inhibitor KCN (to ~ 17%) (Table 1), indicating that the measured activity was specific to bo_3-Qox. A mutant lacking bo_3-Qox (Δbo_3) had ~ 2% of O_2 consumption activity that decreased by one half upon addition of either Na_2S or KCN.

In comparison, the Δ*yhjE*, Δ*ydiM* and Δ*yfcJ* mutants (in the bd^- bo_3^+ background) exhibited highly decreased activities corresponding to ~ 8%, 4% and 5% compared to the parental strain, and similarly, these activities were inhibited drastically by the addition of Na_2S or KCN (Table 1). The data showed that in the absence of the MFS-type transporters YhjE, YdiM, or YfcJ the bo_3-Qox activity was drastically reduced, consequently impairing aerobic growth in the absence of the two *bd*-Qox enzymes. As expected, when the Δbo_3 strain carried a plasmid born copy of *cyoABCDE* (pJRhisA) (14, 68) its bo_3-Qox activity was restored (~ 118.5% ± 6.12), and the bo_3^+ strain carrying the same plasmid overproduced (~ 132.3% ± 0.31) bo_3-Qox activity compared to the bo_3^+ parental wild-type strain [14,68]. Increased bo_3-Qox activity was observed in the Δ*yhjE* (87.0% ± 5.01) or Δ*ydiM* (49.11% ± 2.4) or Δ*yfcJ* (~ 91.17% ± 6.96) mutants when they carried the plasmid pJRHisA, and their aerobic growth defects were at least partially palliated, yielding increased enzymatic activities in all cases (Table 1). In agreement with the earlier transcription profiles, RT-PCR data also indicated that that the plasmid-borne *cyoABCDE* sustained transcription at later stages of growth (OD_{600} of 0.15 or above) (**S2 Fig,** right side).

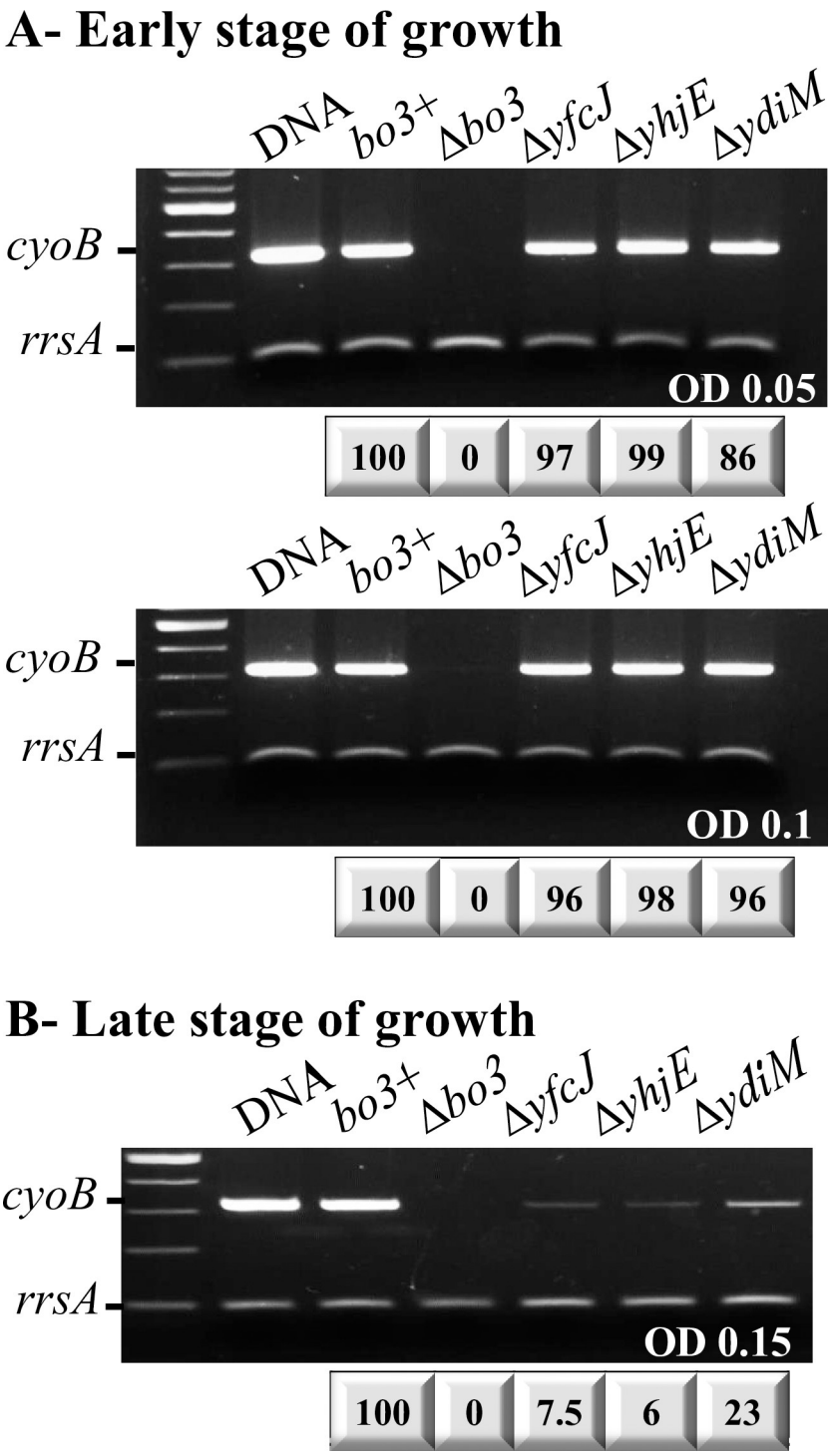

Fig 2. Effects of the absence of YfcJ, YhjE, and YdiM on the transcription of bo_3-Qox. One step RT-PCR was performed on total RNA extract from bo_3^+ strain as well as Δbo_3 (*cyoB*), Δ*yfcJ*, Δ*yhjE*, and Δ*ydiM* mutants using the *cyoB* primers to amplify a 322 bp DNA fragment, and the *rrsA* primers to amplify a 100 bp region of the 16S ribosomal mRNA as a control (Materials and Methods). (**A**) Early stage of growth. The cells were grown under aerobic conditions at OD_{600} of 0.05 (top panel) and 0.1 (bottom panel) where cell division continues. The transcription of *cyoB* was readily detected and showed no difference at both OD_{600}. (**B**) Late stage of growth. The cells were grown under aerobic conditions at OD_{600} of 0.15 (maximum OD_{600} reached). The transcripts of *cyoB* gene were barely detectable when the bo_3-Qox or the MFS-type transporters YfcJ, YhjE, and YdiM are absent. The numbers below each panel indicate the intensities of the corresponding bands, normalized to that of *rrsA* then compared to that seen with the

bo_3^+ strain (taken as 100%). These intensities were determined using ImageJ software (NIH). A control PCR where the reverse transcriptase enzyme was inactivated at 95˚C was performed for each total RNA extract to check for DNA contamination. Each experiment is repeated at least three times, and a representative sample is shown for each case.

https://doi.org/10.1371/journal.pone.0293015.g002

Absence of YhjE, YdiM, or YfcJ affects the heme composition of bo_3-Qox

The dithionite-reduced *minus* ferricyanide-oxidized optical difference spectra was obtained using membrane fractions of appropriate *E. coli* mutants grown at an early stage of growth to monitor their *b*- and *o*-type heme compositions. The data indicated that the membranes of the bo_3^+ strain or its derivative overproducing bo_3-Qox (bo_3^+ + pJRhisA), showed a broad band centered at 560 nm with a shoulder at ~ 563 nm (Fig 3), characteristic of the presence of the *b* and o_3 hemes of bo_3-Qox [69]. In the Δbo_3 strain this band was drastically reduced, consistent with the absence of the bo_3-Qox. The remaining small amounts of absorbance likely reflected possible contamination from the abundant periplasmic cyt b_{562}. Similarly, the membranes of Δ*yfcJ*, Δ*yhjE*, or Δ*ydiM* mutants exhibited trace amount of heme *b* and o_3 spectra (Fig 3), confirming that in the absence of either YfcJ, YhjE, or YdiM the *b*- and *o*-type hemes of bo_3-Qox were undetectable despite the presence of *cyoABCD* mRNA, and consistent with the absence of the enzyme activity and defective aerobic growth (Table 1). The overall data indicate that the absence of either YhjE, YdiM, or YfcJ abolishes the production of an active bo_3-Qox enzyme when this enzyme is expressed from a chromosomal copy, whereas the effect(s) of these UMFs was still apparent but less pronounced when the *cyoABCDE* operon was

Table 1. The bo_3-Qox activity of various strains.

Strains	UQ1	UQ1+ Na_2S	UQ1+ KCN
[a]bo_3^+	[a]100 ± 3.5	[c]14.7 ± 2.8	[c]17.0 ± 2.9
Δbo_3	2.2 ± 0.2	0.7 ± 0.2	0.5 ± 2.3
Δ*yfcJ*	7.9 ± 3.1	1.1 ± 2.3	1.5 ± 1.1
Δ*yhjE*	4.3 ± 1.1	1.8 ± 0.2	1.4 ± 0.6
Δ*ydiM*	5.0 ± 0.7	0.5 ± 0.6	2.7 ± 0.7
[b]bo_3^+ + pJRhisA	[b]132.3 ± 0.3	22.7 ± 0.7	26.3 ± 1.7
Δbo_3 + pJRhisA	118.5 ± 6.1	13.9 ± 1.8	19.0 ± 0.5
Δ*yfcJ* + pJRhisA	91.1 ± 7.0	11.5 ± 1.0	21. 8 ± 4.3
Δ*yhjE* + pJRhisA	87.0 ± 5.0	6.6 ± 2.5	15.3 ± 4.4
Δ*ydiM* +pJRhisA	49.1 ± 2.4	3.8 ± 0.9	8.3 ± 3.7

The bo_3-Cox activities were measured by monitoring the oxygen consumption activities of whole cells using a Clark-type oxygen electrode. The activities were measured by incubating ubiquinol-1 (UQ1) with sodium dithionate at 30˚ C prior to adding the cells (see **Materials and Methods**) and all the assays were performed at least three times, with the p values being <0.05 for all mutants.

[a]The parental bo_3^+ strain exhibited ~ 34 mmoles of O_2 consumed/min/OD_{600} of cells and taken as 100%.

[b]+ pJRhisA refers to the complementation of various mutants with a plasmid harboring bo_3-Qox operon [14].

[c]10 μM of sodium disulfide (Na_2S) or 200 μM of potassium cyanide (KCN) were used to inhibit the bo_3-Qox activity, as needed.

https://doi.org/10.1371/journal.pone.0293015.t001

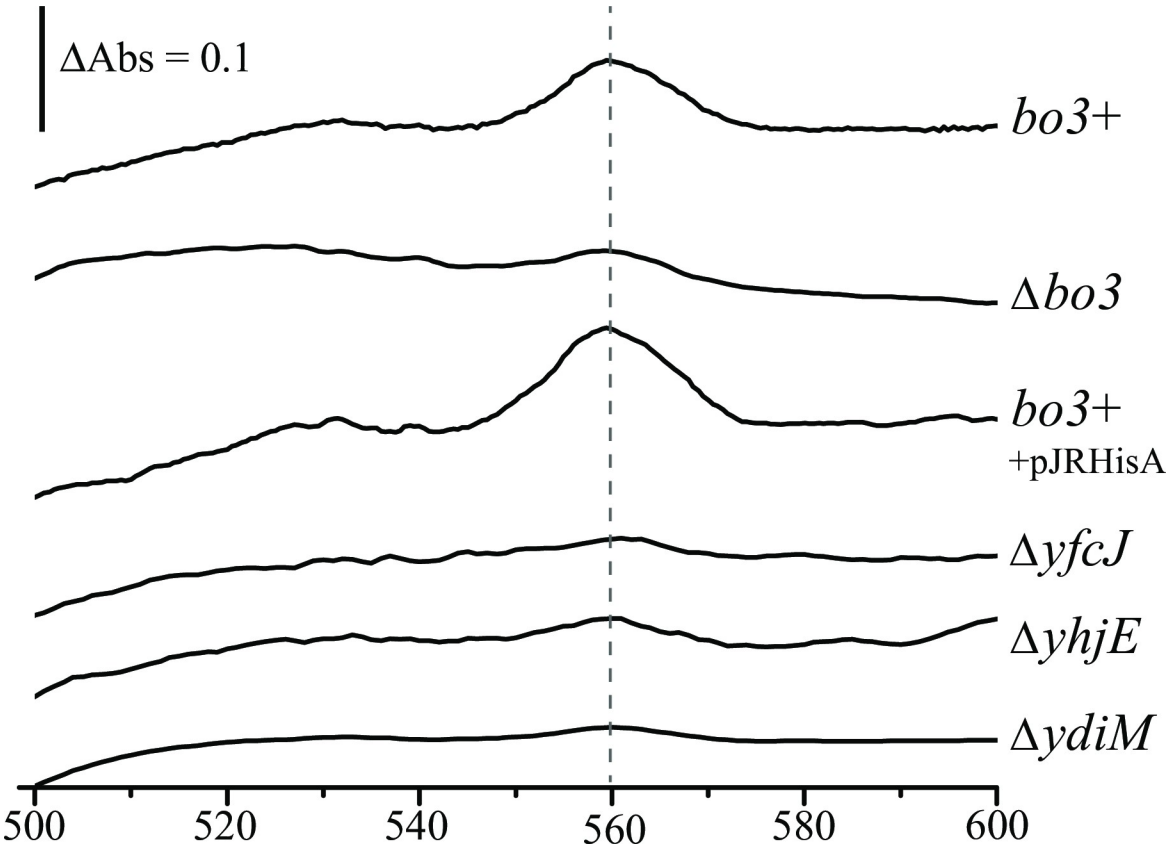

Fig 3. *b*-type heme compositions of the Δ*yfcJ*, Δ*yhjE*, and Δ*ydiM* mutants. The reduced *minus* oxidized spectra of the membranes prepared from the bo_3^+ strain as well as the Δbo_3, Δ*yfcJ*, Δ*yhjE*, and Δ*ydiM* mutants grown under aerobic condition at an OD_{600} of 0.1. The *bd*-Qox1 and *bd*-Qox2 being absent, the observed broad peak at 560 nm in bo_3^+ and the strain overproducing bo_3-Qox (bo_3^+ + pJRHisA) was taken as corresponding to the hemes *b* and o_3 of bo_3-Qox. This peak is drastically reduced in Δbo_3 as well as the Δ*yfcJ*, Δ*yhjE*, and Δ*ydiM* strains. Each experiment is repeated at least three times, and a representative sample is shown for each case.

https://doi.org/10.1371/journal.pone.0293015.g003

overexpressed from the multicopy plasmid pJRHisA. Combined with the RT-PCR assays, these results suggest that the negative impact of the Δ*yhjE*, Δ*ydiM*, and Δ*yfcJ* mutants on bo_3-Qox gene expression does not fully explain the complete loss of activity of bo_3-Qox.

Cellular ^{64}Cu or ^{55}Fe uptake by mutants lacking either YhjE or YdiM or YcfJ

The *E. coli* bo_3-Qox is a heme-Cu containing enzyme, and some members of MFS-type transporters transport Cu (*e.g.*, CalT family members) [46,47,49] or Fe [70] or siderophores [71,72]. Thus, the Δ*yhjE*, Δ*ydiM* and Δ*yfcJ* derivatives of an otherwise wild-type strain (BW25113) were assessed for their abilities to take up radioactive ^{64}Cu or ^{55}Fe using whole cells at an early stage of their growth (OD_{600} of 0.1).

In the case of Cu, *E. coli* wild-type cells (BW25113) showed robust, time dependent and temperature sensitive (35˚ C *versus* 4˚ C) ^{64}Cu uptake kinetics (**Fig 4A**). Under the same conditions, the Δ*yfcJ* and Δ*yhjE* mutants behaved like a wild-type strain in respect to ^{64}Cu uptake kinetics, indicating that the absence of YfcJ or YhjE had no effect on cellular Cu accumulation. The Δ*cyoB* strain exhibited reduced ^{64}Cu uptake kinetics, suggesting that in the absence of bo_3-Qox, the main cupro-enzyme present in *E. coli*, cellular Cu accumulation decreased, possibly due to Cu homeostasis. Remarkably, the Δ*ydiM* mutant also exhibited slow ^{64}Cu uptake

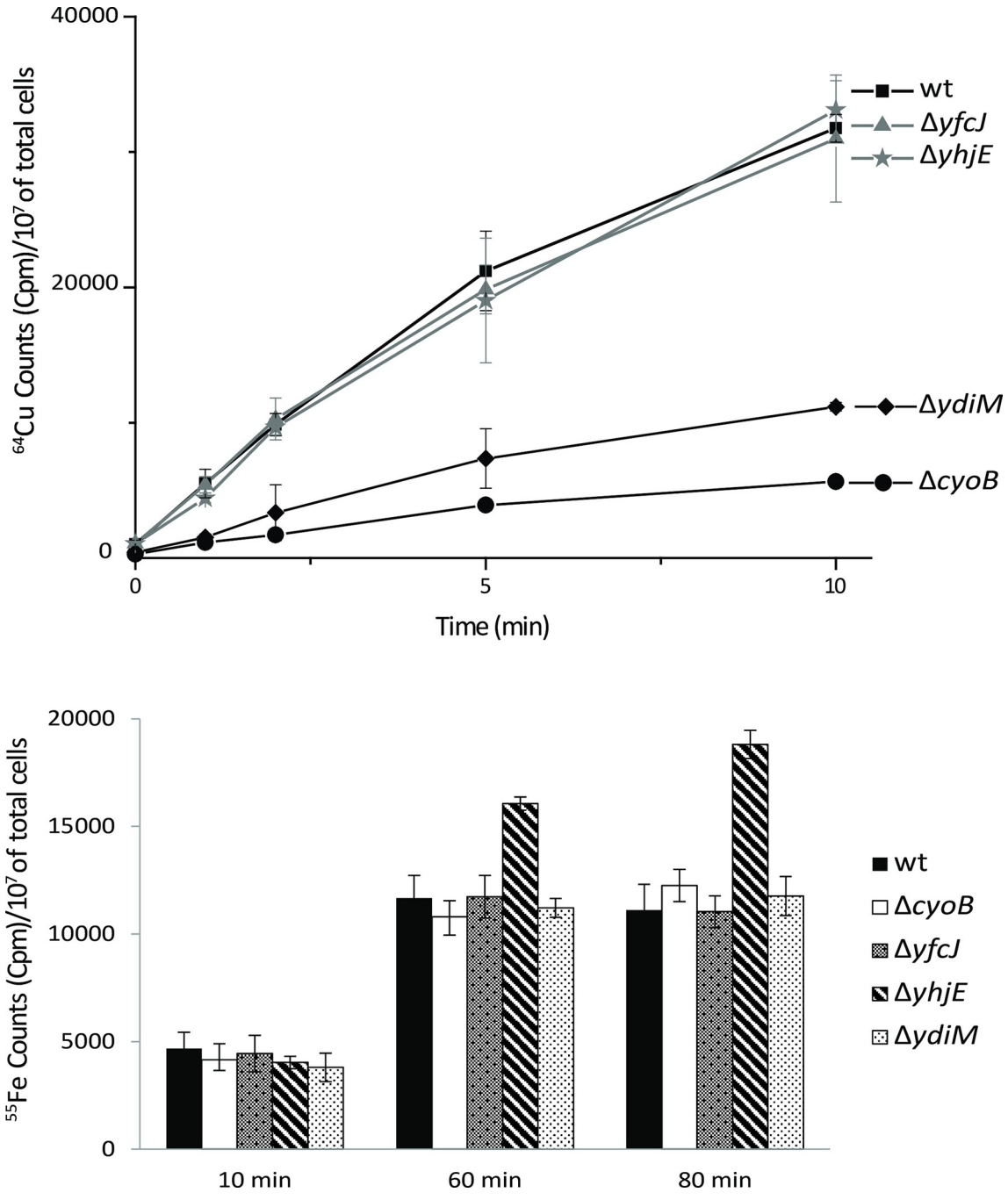

Fig 4. Whole cell radioactive ^{64}Cu and ^{55}Fe uptake kinetics of the Δ*cyo*, Δ*yfcJ*, Δ*yhjE*, and Δ*ydiM* mutants. ^{64}Cu (top panel) and ^{55}Fe (bottom panel) uptake kinetics (Materials and Methods) were carried out at 35˚C using whole cells grown aerobically until an OD_{600} of 0.1. In each case, the uptake assays were repeated at least three times using at least three independently grown cells, and the p values were > 0.05 The Δ*ydiM* and Δ*yhjE* mutants shows lower ^{64}Cu ($p < 0.05$) and higher ^{55}Fe ($p < 0.05$) accumulations in cells, respectively.

https://doi.org/10.1371/journal.pone.0293015.g004

kinetics (Fig 4A) compared with it parental strain, indicating that cellular Cu accumulation decreased. This behavior was reminiscent to that observed with the *R. capsulatus ccoA* mutant that is defective in ^{64}Cu uptake [47]. As controls, when the assays were performed at 4˚ C, all strains showed greatly reduced rates of ^{64}Cu uptake.

In the case of Fe, the uptake of ^{55}Fe-sodium ascorbate (*i.e.*, reduced iron) followed similar kinetics for the wild type and the *DycfJ* and *DydiM* mutants, except the Δ*yhjE* strain that accumulated higher amounts of cellular ^{55}Fe (Fig 4B). Since the assays report the net accumulation of the radioisotope used (*i.e.*, total import *minus* total export during a given incubation period), the data suggested that the Δ*yhjE* was either overactive for import, or deficient for export, of cellular Fe leading to gradual accumulation over the time (Fig 4B). As in the case of Cu, when the Fe uptake assays were performed at 4˚ C, very reduced ^{55}Fe uptake rates were observed. Further, when uptake assays were performed without prior incubation of ^{55}Fe with sodium ascorbate (*i.e.*, with oxidized form of ^{55}Fe), then all strains including the Δ*yhjE* exhibited comparable ^{55}Fe uptake activities. Thus, YhjE affected the transport of reduced, but not oxidized, form of Fe. Overall, whole cells uptake kinetics indicated that the absence of YdiM and YhjE perturbs Cu and Fe homeostasis, respectively, in *E. coli* cells. How the cellular imbalance of Cu or Fe in mutants lacking these two MFS-type transporters is linked to the observed bo_3-Qox deficiency and aerobic growth defect, requires further studies.

YhjE is related to the putative hydroxy-ethyl-thiazol (HET) and other transporters that cluster with bo_3-Qox

YhjE (TC: 2.A.1.6.10) belongs to a large subfamily of the MFS-type transporters with homologues in most major bacterial phyla. In TCDB, YhjE is listed as a metabolite:H+ symporter (MHS) family member, but its metabolite cargo is unknown. YhjE homologues are identified in beta- and alpha-proteobacteria in addition to gamma-proteobacteria, with sequence similarity hits (based on top 1000 blastP hits against UniProt reference proteomes) being predominately related to proteins from the Proteobacteria (49%) and Actinobacteria (43%). A sequence similarity network analysis indicates that of the previously published MFS-type transporters, YhjE is most similar to ThiU [73] (TC 2.A.1.6.12; putative thiazol transporter according to TCDB) (Fig 5A) (S4 Fig). Based on previous gene clustering and phylogenetic profiling analyses, ThiU is predicted to be a hydroxy-ethyl-thiazole (HET) transporter required for thiamin biosynthesis [73], although this hypothesis has not been tested experimentally. Based on phylogenetic reconstruction, ThiU and YhjE may be paralogs, suggesting that ThiU and YhjE could have separate functions (Fig 5A). As an example, the *Haemophilus influenzae* genome encodes a ThiU ortholog (HI_0418) located in the thiamine-related genes cluster, and a YhjE ortholog (HI_0281) next to two genes encoding enzymes involved in menaquinone biosynthesis (2-succinyl-6-hydroxy-2, 4-cyclohexadiene-1-carboxylate synthase/ 2-oxoglutarate decarboxylase (MenD; HI_0283) and menaquinone-specific isochorismate synthase (MenF; HI_0285). Intriguingly, MenD is a thiamine-dependent protein. (Fig 5A). However, this proximity between a gene encoding YhjE-like proteins and a gene encoding MenD is only observed in *Haemophilus* species.

Noticeably, YhjE-like proteins are identified in some Proteobacterial genomes that are encoded by genes next to the *cyoABCD* operons, encoding the structural subunits of bo_3-Qox (Fig 5B). Except for the gene clusters from Thiotrichales, Chromatiales, and Hyphomicrobiales, where the *yhjE*-like gene is in the same operon with *cyoABCD*, most *yhjE*-like genes are found in the opposite orientation, suggesting that although *yhjE* and *cyoABCD* may not form an operon, still they might be co-regulated (Fig 5C). These YhjE-like proteins, although not connected to the main sequence similarity network cluster (*i.e.*, have an $E_{value} > 1E\text{-}70$ with any other protein in the main cluster), might be closely related to YhjE in the phylogenetic tree (Fig 5B). This observation suggests that the role of YhjE in bo_3-Qox function is likely conserved outside of *E. coli*.

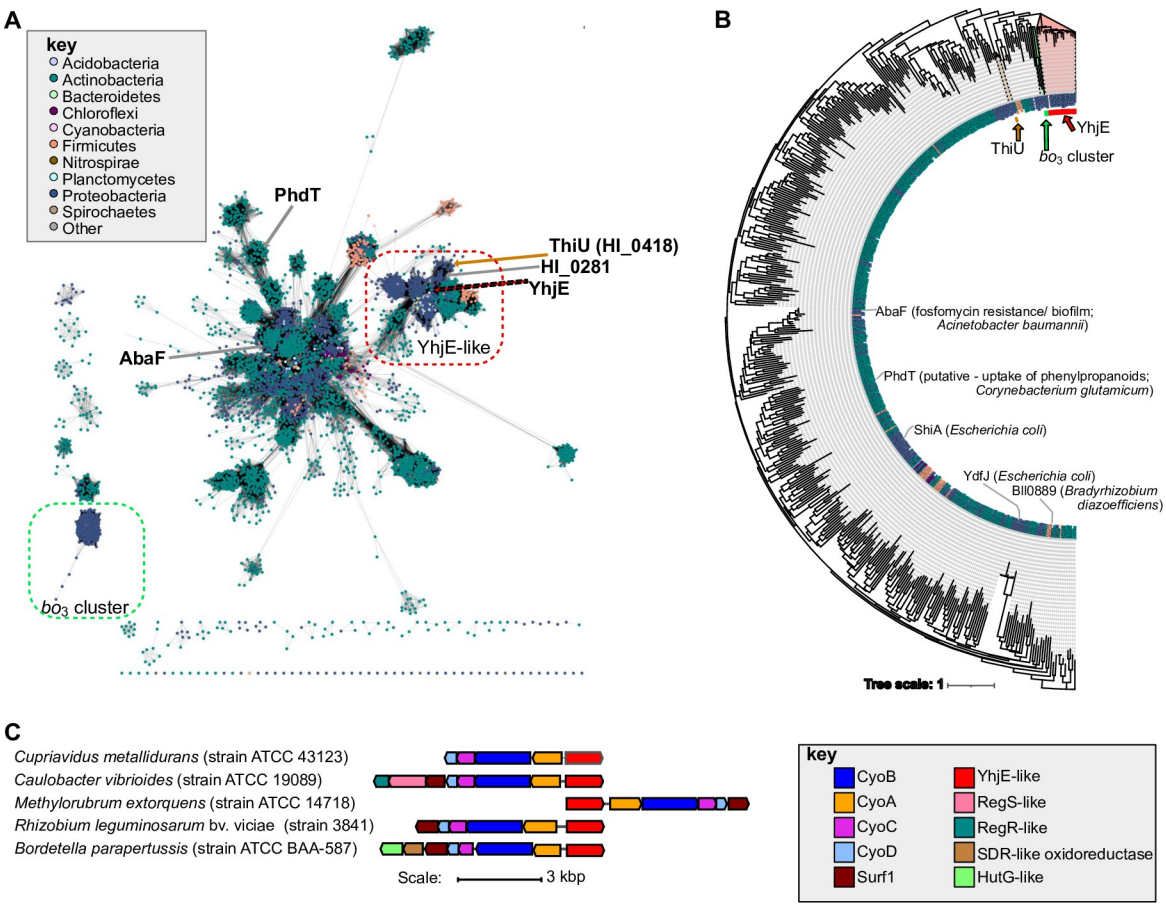

Fig 5. Sequence similarity analysis of YhjE-like transporters and gene neighborhoods containing its homologues. (**A**) Sequence similarity network using an alignment score of 110. Sequences for the network were collected by searching against UniRef50 (500 hits) with YhjE and mapping to UniRef90 for network construction. Experimentally characterized proteins or proteins with predicted functions (in italics) based on bioinformatic analyses are labeled. The taxonomic classification of each node is colored according to the key shown on top left. (**B**) iqTREE using edited MAFFT alignment based on UniRef50 sequences, and (**C**) examples of gene neighborhoods containing a YhjE-like MFS transporter with the key defining them located at the bottom right.

https://doi.org/10.1371/journal.pone.0293015.g005

The ydiM-like genes are linked to the shikimate pathway

In the *E. coli* K-12 genome, *ydiM* (TC: 2.A.1.15.12) is located next to its paralog *ydiN* (TC: 2.A.1.15.13), and two other genes encoding two enzymes in the shikimate pathway, *aroD* and *ydiB*, encoding 3-dehydroquinate dehydratase and quinate/shikimate dehydrogenase enzymes, respectively. The shikimate pathway is a major link between carbohydrate metabolism and the biosynthesis of aromatic compounds via chorismate, a precursor of aromatic amino acids phenylalanine, tyrosine, and tryptophan. The cargo of YdiN is not listed in TCDB, but it was previously hypothesized to transport a shikimate by-product [74] based on the genomic context and co-expression data of the *ydiN*, *aroD*, and *ydiB* genes. YdiM is listed as a putative isoprenol exporter due to increase susceptibility that it provides to *E. coli* upon its deletion [75].

Phylogenetic and genomic context analyses of YdiM and YdiN homologues further defined their relationship to the shikimate pathway. The YdiM and the YdiN orthologous group are largely limited to Enterobacterales genomes and not widespread in Proteobacteria. YdiM/YdiN-like proteins are frequently found in Firmicute genomes, represented by YfkL in *Bacillus subtilis* (**Fig 6**). Accordingly, among YdiM homologues (top 1000 blastP hits) ~ 57% are from

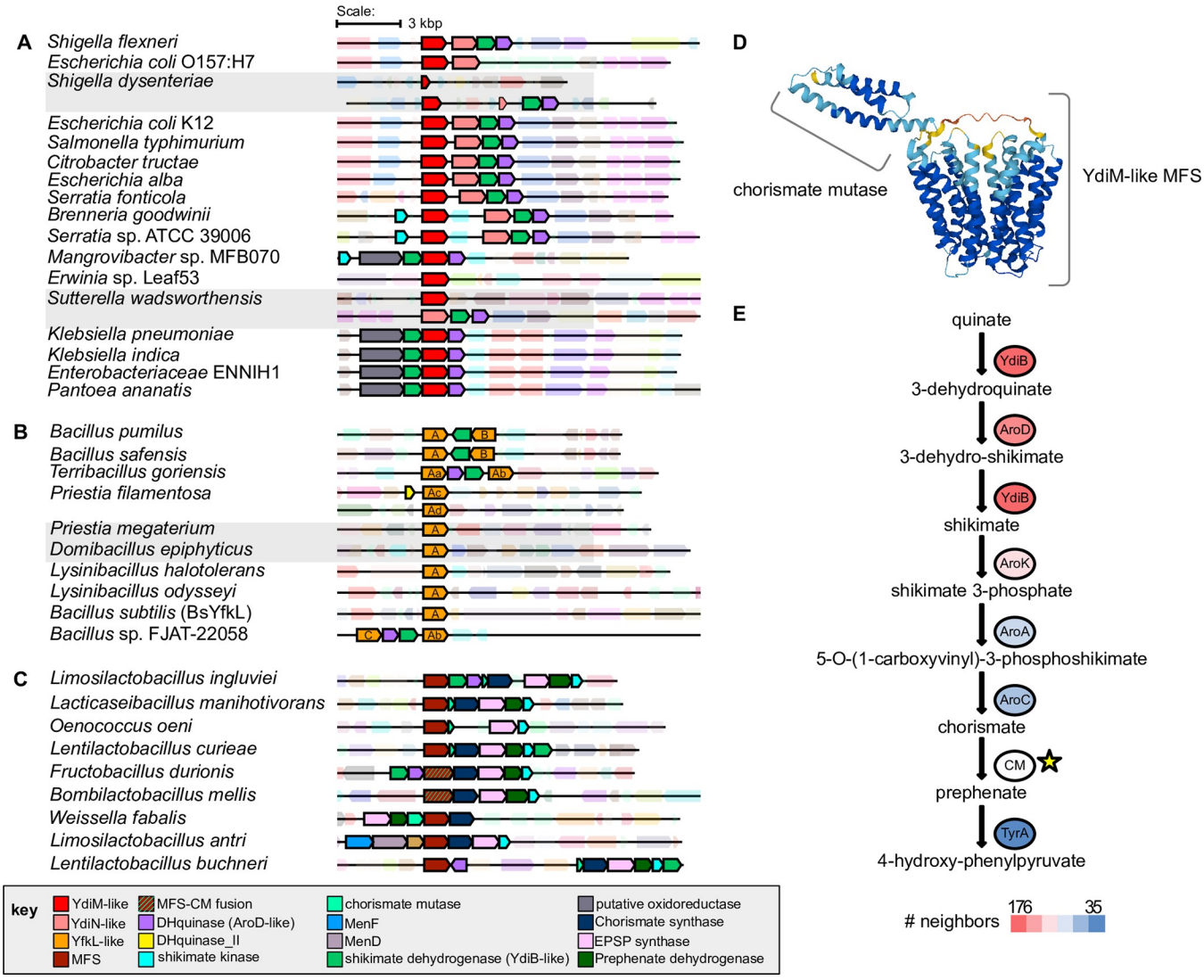

Fig 6. Phylogenomic analysis of the YdiM/YdiN subfamily. (**A**) Phylogenetic tree of YdiM, YdiN, and their YdmiM-like and YdiN-like homologues. The taxonomic classification of each leaf, presence of the chorismite mutase fusion, and whether the corresponding gene is next to a gene encoding a shikimate pathway enzyme are indicated with inner rings according to the key shown at the bottom of the figure. Lines colored by taxonomic classification connecting two leaves are used to indicate that those two proteins are encoded by the same genome. The innermost grey ring corresponds to the clusters depicted in panel B, and YfkL indicates the homologue present in *Bacillus subtilus* (Bs). Gene neighborhoods from clades with background shading are shown in Fig 6. Sequences are the 250 best hit from blastp against UniProt reference proteomes. The 10 most similar proteins to YdiM in *E. coli*, *Clostridioides difficile*, *Klebsiella pneumoniae*, *Bacillus subtilis* were used as an outgroup to root the tree. (**B**) Sequence similarity network (SSN) of YdiM/YdiN homologues. Nodes are colored by taxonomy according to the key shown at the bottom of the figure, and clusters are labeled as in the innermost grey ring of panel A. Edge-weighted Spring Embedded Layouts using % id for clustering. (**C**) SSN as in panel B but colored based on presence of neighbor gene(s) encoding enzyme(s) in the shikimate pathway, and (**D**) shows the nodes in red representing the YdiM orthologs with a chorismate mutase fusion.

https://doi.org/10.1371/journal.pone.0293015.g006

Firmicutes and ~ 23% are from Proteobacteria. Remarkably, ~ 75% of YdiM/YdiN homologues analyzed here are encoded by a gene that is adjacent (on either the 5' or 3' side) to a gene encoding an enzyme in the shikimate pathway (Fig 6). Moreover, this frequency increases to ~ 86% when a larger (20 instead of the usual 10) genes window is used, showing a clear link between the YdiM and YdiN subfamily of the MFS-type transporters and the enzymes of the shikimate pathway (Fig 7). In addition to *E. coli*, other Enterobacteriaceae genomes including *Shigella flexneri*, *Salmonella typhimurium*, and *Citrobacter tructae* also

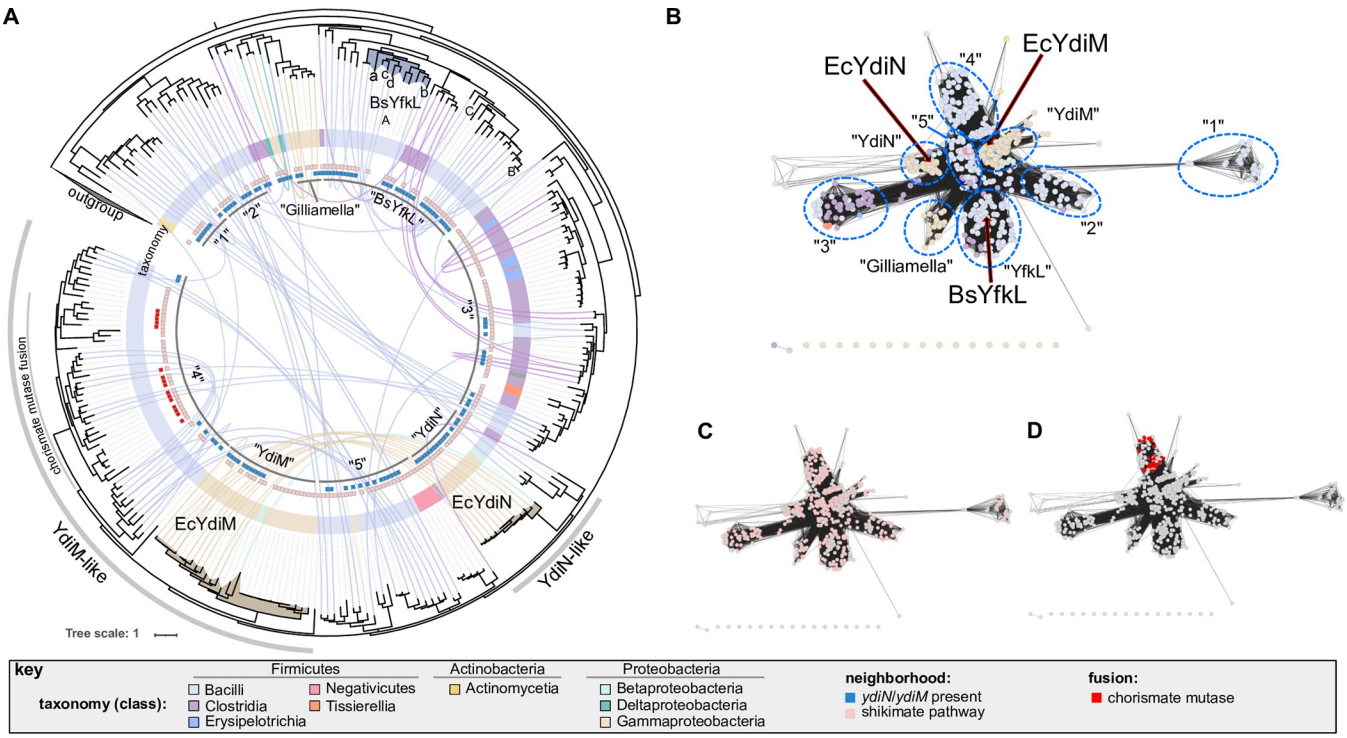

Fig 7. Gene neighborhoods containing *ydiM*/*ydiN* homologues. (**A**) Gene neighborhoods of the YdiM and (**B**) gene neighborhoods of the YdiN clades. (**C**) Representatives from Cluster 4 shown in Fig 5. (**D**) Alphafold prediction depicting the YdiM-chorismate mutase fusion from *Fructobacillus durionis*, showing its two distinct domains. (**E**) Shikimate pathway from quinate to 4-hydroxy-phenylpyruvate and the structural genes of the enzymes involved. A star indicates the step catalyzed by chorismite mutase (CM) that is sometimes found fused to YdiM as shown in (D). The number of times a YdiM/YdiN homologue is encoded in a gene neighborhood with a gene encoding the indicated enzyme is shown as a heatmap (176 red to 35 blue).

https://doi.org/10.1371/journal.pone.0293015.g007

encode both YdiM and YdiN located next to the shikimate pathway genes *ydiB* and *aroD* (**Figs 6** and 7). However, *Klebsiella pneumoniae* encodes only YdiM, and in such Enterobacterial genomes that lack a YdiN ortholog, *ydiM* is found between *aroD* and *ydiB* in a putative operon (**Fig 7A**), further linking YdiM with the shikimate pathway. Moreover, in multiple Firmicutes *ydiM* genes encoding YdiM orthologs are often physically located next to genes encoding shikimate pathway enzymes (**Fig 7B**), and even in a handful of cases, the YdiM orthologs are fused to chorismate mutase (**Fig 7C and 7D**). Chorismate mutase is one of the seven enzymes that form the shikimate pathway (**Fig 7E**) and is often found fused to other enzymes of this pathway and thought to serve regulatory purposes [76]. Of the genes analyzed here, *ydiM* and *ydiN* homologues are most often near the enzymes catalyzing the early steps of the shikimate pathway, starting from quinate (*i.e.*, *ydiB*>*aroD*>*aroK*) compared to others operating in the pathway (**Fig 7E**). The overall findings indicated that the YdiM-like proteins are closely associated with the shikimate pathway, and consistent with YdiM and YdiN performing different transport function(s) related to the aromatic acid synthesis pathway.

Bioinformatic analysis of YfcJ-like proteins

Currently little is known about YfcJ (TC: 2.A.1.46.6) and its homologues. The closest related protein with some associated experimental data is YhhS (TC: 2.A.1.46.7), a paralog of YfcJ in *E. coli*, which was previously linked to cellular arabinose levels [77] and glyophosate (inhibitor of 5-enolpyruvylshikimate-3-phosphate synthase) resistance [78] based on loss-of-function and gain-of-function experiments, respectively. The sequence similarity network and

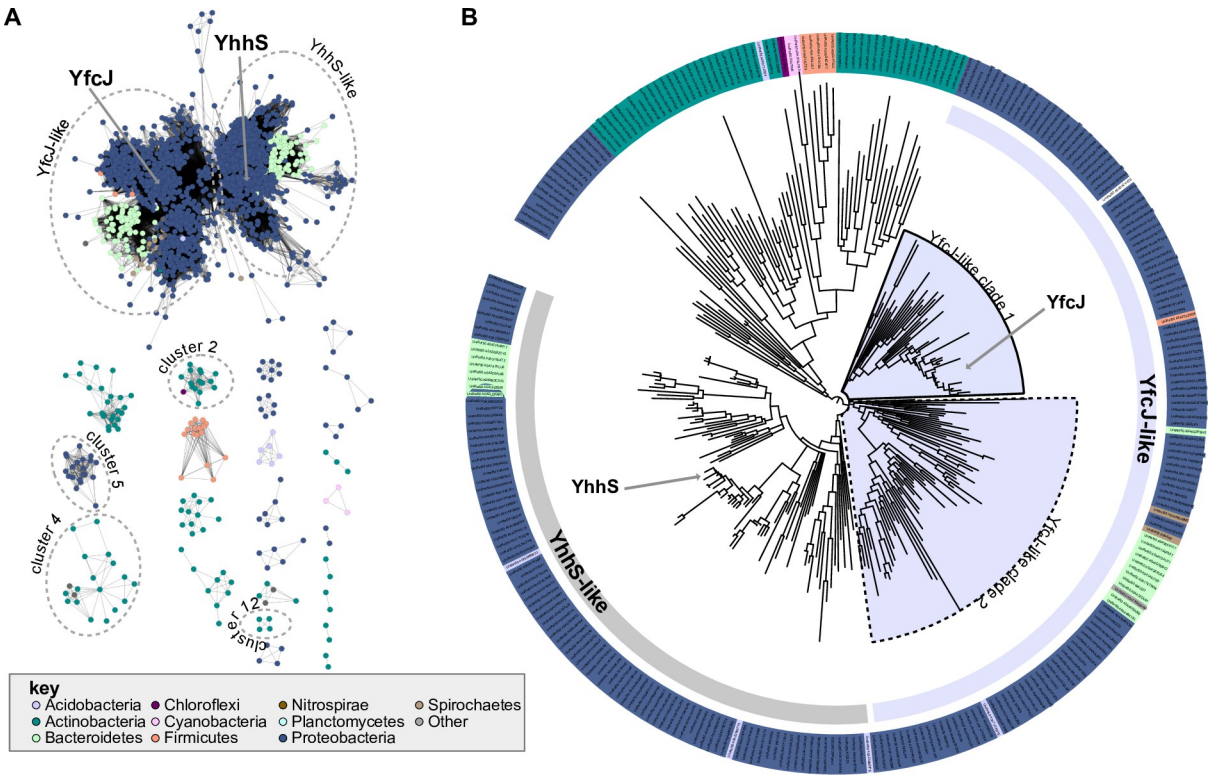

Fig 8. Sequence similarity analysis of YfcJ homologues. (**A**) Sequence similarity network using an alignment score of 80. Sequences for the network were collected by searching against UniProt using YfcJ as a query. Clusters with examples of gene proximity in Fig 9 are circled and labeled. The taxonomic classification of each node is colored according to the key shown at the bottom left of the figure. (**B**) Protein sequences from the network were mapped to UniRef50 and representative nodes were used to build a phylogenetic tree. The background color of each leaf is colored according to the key. In addition to clear separation from the YhhS-like clade, the YfcJ group can be distinguished into two major clades, indicated as YfcL-like clade 1 and clade 2.

https://doi.org/10.1371/journal.pone.0293015.g008

phylogenetic reconstruction analyses were able to distinguish the YfcJ-like homologues from the closest subfamily composed of YhhS homologues. (**Fig 8A and 8B**). The YfcJ-like subfamily was mainly identified in Proteobacteria and Bacteroidetes (89% and 8.5% of the homologs, respectively), and within the Proteobacteria, there was a roughly equal split between gamma- (30%), alpha- (30%), and beta- (27%) proteobacteria. Analysis of conserved gene proximity revealed multiple putative operons encoding YfcJ- and YhhS-like transporters. Although defined biochemical functions could readily predicted for proteins encoded by genes neighboring the *yfcJ* homologues, such as amidohydrolases or tautomerases, no specific pathway or process that may be associated with YfcJ could be predicted (**Fig 9**, upper part). Note that the clusters 4, 5, and 12 of YhhS homologues are in putative operons with nucleotide metabolism and tRNA-related proteins, linking the YhhS family to nucleotide metabolism and tRNA modification processes based on conserved gene proximity (**Fig 9**, lower part). Of these clusters, the genes in cluster 4, which is dominated by Actinobacteria, are often in a putative operon with a YacP-like endoribonuclease, and a protein resembling an epoxyqueuosine reductase responsible for a synthesis of queuosine found in some tRNAs. Cluster 5 from Proteobacteria is found in a putative operon with proteins involved in nucleotide metabolism, including a putative hydrolase from the YjjG superfamily involved in cleaving nucleotides with non-canonical nucleotide bases. In cluster 12 the YfcJ- and YhhS-like homologues are in a putative operon with glutamyl-Q tRNA (Asp) synthetase, which is a protein that functions immediately

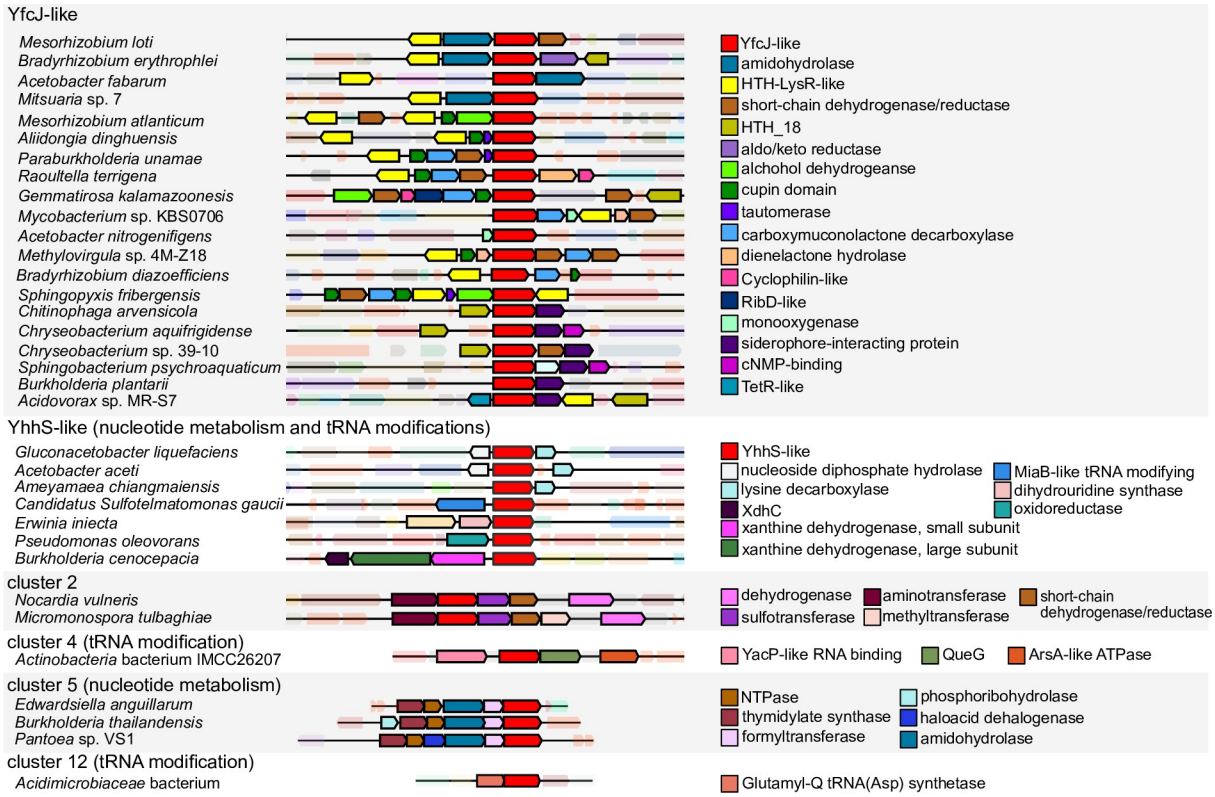

Fig 9. Conserved gene proximity analysis of YfcJ homologues. Examples of conserved gene neighborhoods encoding proteins from the YfcJ sequence similarity network are shown. Clusters corresponding to genes involved in nucleotide metabolism and tRNA modification (YhhS-like). tRNA modification (cluster 4), nucleotide metabolism (cluster 5) and tRNA modification (cluster 12) are shown with the related enzymes found shown on the right.

https://doi.org/10.1371/journal.pone.0293015.g009

downstream of epoxyqueuosine reductase involved in the synthesis of the hypermodified base glutamyl-queuosine [79]. For cluster 2 in the network, which is largely confined to Actinobacteria, all YfcJ- and YhhS-like homologues are encoded by a gene that is potentially in a biosynthetic gene cluster for an unknown secondary metabolite, suggesting that they may be metabolite transporters.

Discussion

The MFS-type transporter CcoA (TC: 2.A.1.81.1) of the CalT subfamily is a well-established Cu importer identified in bacteria and required for biogenesis of the cbb_3-Cox Cu_B center [11,46,49]. However, although CcoA is widespread among alpha-proteobacterial species and it frequently co-occurs with the genes encoding aa_3-Cox and cbb_3-Cox [48,49], it is only required for cbb_3-Cox and not the quasi-identical Cu_B center containing aa_3-Cox, as seen with *R. sphaeroides* [49]. Moreover, no functional ortholog of *R. capsulatus* CcoA is found among the ~ 70 MFS-type transporter genes of *E. coli*, suggesting a different mechanism for Cu import and biogenesis for the bo_3-Cox Cu_B center. These observations point out the specificity of the CalT members among the MFS-type transporters and indicate the possible occurrence of different routes for the biogenesis of Cu_B centers of heme-Cu enzymes (*e.g.*, *E. coli* bo_3-Cox). Indeed, bacterial cbb_3-Cox and aa_3-Cox require specific transporters and chaperones for the biogenesis of their Cu_B centers assembly, including the periplasmic Sco-like [31,35] and PCuAC-like chaperones [2,32,33,38]. Moreover, cbb_3-Cox requires in addition to the Cu

importer CcoA [46] the cupric reductase CcoG [43], and the P_{1B}-type transporter CcoI/CtpA [26,44,45]. Remarkably, none of the latter proteins are involved in the case of the aa_3-Cox, which instead uses the Cu chaperone Cox11 [36–38]. How the Cu_B center insertion occurs in *E. coli* bo_3-Qox is not known, and as a true CalT homologue does not seem to exist in this species, raising the issue of whether any other type of MFS-transporter might accomplish this function.

A survey of the *E. coli* genome indicated that among the ~ 70 MFS-type transporters, ~ 28 of them (*i.e.*, UMFs) had no identified cargo, and at least eight of them were richly endowed with plausible metal-coordinating amino acid residues. This enticed us to examine the role of these UMFs in bo_3-Cox biogenesis, using a genetic screen based on the essentiality for aerobic respiratory growth sustained by this enzyme in the absence the *bd*-Qox1 and *bd*-Qox2. This screen identified YhjE, YdiM, and YfcJ as required MFS-type transporters for bo_3-Cox dependent aerobic respiratory growth of *E. coli*. In the absence of any one of these proteins, the bo_3-Qox activity and its *b*- and o-type hemes were absent, even though at low cell-densities detectable amounts of *cyoABCD* mRNA transcripts were produced. Remarkably, a multicopy plasmid carrying these genes and overproducing the bo_3-Qox could bypass at least partially the need for these UMFs. These findings suggested that some regulatory event(s) (*e.g.*, titrating out a regulator) controlling the transcription or destabilizing the transcript(s) might occur in the absence of these UMFs. Alternatively, although these mutants might produce the structural constituents of the bo_3-Qox, they could not assemble an active enzyme in the absence of the imported/exported cargo(s). Thus, the specific nature(s) of currently unidentified cargos transported by these MFS-type transporters seem important for bo_3-Qox biogenesis. Earlier genetic studies have suggested that *yhjE*, *ydiM*, and *ycfJ* may be involved in transporting an unknown metabolite (see TCDB), isoprenol [75] and arabinose [77], respectively. Here, the whole-cell transport assays further showed that cells without YdiM accumulated less ^{64}Cu, and those without YhjE contained more reduced ^{55}Fe (**Fig 4**), while no such difference was seen in the absence of YfcJ. Note that currently no conclusive data exist for any of these transporters, as none of them has been purified and shown to bind and transport their putative substrates.

Bioinformatics analysis have been performed to unravel the function of YfcJ, YhjE and YdiM. No link between bo_3-Qox and metal transport were found for YfcJ. YhjE was referred to as a member of the metabolite: H+ symporter (MHS) Family (see TCDB), and phylogenomic analyses show that in many bacterial genomes, *yhjE* gene clusters with the bo_3-Qox structural genes *cyoABCD*, suggesting that the role of YhjE-like transporters in bo_3-Qox function could be widely conserved (**Fig 7**). Based on an analysis of previously published high-throughput (HTP) interaction data [80], YhjE was found to physically interact with FhuA, a ferrichrome outer membrane transporter [81]. Out of 331 identified genetic interactions in a separate study, a positive genetic interaction was identified with *fhuA* (*i.e.*, the double *yhjE fhuA* mutant grew better in rich medium than the single mutants), and negative genetic interactions with other Fe transporters (*fecA*, *fecB*, *fecC*, *fecD*, *fepA*, *fepB*, *febD*, *fes*, and *fhuC*) [80]. If these results obtained with HTP studies are not misleading false positives, they could potentially explain the Fe-homeostasis defect in the Δ*yhjE* strain. A negative genetic interaction was also observed between *yhjE* and *cyoA* or *cyoB* and a positive genetic interaction with *cyoC*. Such results may suggest that YhjE could have functional roles beyond bo_3-Qox biogenesis. Overall, the available experimental and bioinformatic data support that this transporter is required to produce an active bo_3-Qox, but the underlying molecular link(s) remains unknown.

YdiM was initially selected as a candidate metal transporter based on the presence of $M_{21}XXXXM_{26}$ and $M_{76}XXM_{79}XXXM_{83}$ motifs in its predicted TM1 and TM3, and other motifs in the TM4, and TM6 (**S5 Fig**). The 3D structural model of YdiM is reminiscent of that of CcoA since the Met residues are positioned in a similar fashion throughout the TMs of both

proteins. However, the putative transmembrane metal-binding motif(s) are different from the CalT subfamily members (**S5 Fig**) [11]. These putative metal binding residues combined with the experimental data presented here suggest that YdiM could be a plausible candidate for Cu transport. In the *E. coli* K-12 genome *ydiM* gene and its paralog *ydiN* are clustered together with several genes involved in the shikimate pathway, which is the metabolic pathway governing biosynthesis of aromatic amino acids, like phenylalanine, tyrosine, and tryptophan [82,83]. Phylogenetic analyses of bacterial species other than *E. coli* also indicate that *ydiM* and *ydiN* cluster frequently with the shikimate pathway genes (**Figs 5** and **6**). An earlier study indicated that the 3-deoxy-D-arabino-hepulosonate-7-phosphate synthase (DAHP synthase) catalyzing the first step of this pathway binds Cu, suggesting that the DAHP synthase may be a cuproenzyme [84]. However, no conclusive study has been conducted, leaving the identity of the metal of DAHPS contested [85], and the link between Cu, the shikimate biosynthetic pathway, and bo_3-Qox remains unclear, deserving future studies.

In summary, this study unexpectedly implicated three MFS-type transporters, YhjE, YdiM and YfcJ in the production of an active bo_3-Qox in *E. coli*. Available data showing impaired Cu and Fe uptake kinetics suggest that YdiM and YhjE are involved in cellular metal homeostasis, which may be essential for the biogenesis of the heme-Cu enzyme bo_3-Cox. However, the cargo of these transporters being currently unknown, and their role(s) in specific metabolic pathway(s) undefined, a direct mechanistic link between them and the expression or assembly of the bo_3-type Qox remains hypothetical until such data become available. Nonetheless, the overall findings increased the arsenal of the different gene products that cells use to produce heme-Cu enzymes, including the bo_3-Qox. These studies also illustrated how broad a biological function the MFS-type transporters may play in cells and spur future investigations to identify the transported substrates and shed light to the mechanistic link(s) between these MFS-type transporters and the biogenesis of heme-Cu containing metalloproteins.

Supporting information

S1 Fig.
(PDF)

S2 Fig.
(PDF)

S3 Fig.
(PDF)

S4 Fig.
(PDF)

S5 Fig.
(PDF)

S1 File.
(DOCX)

S1 Dataset.
(XLSX)

Acknowledgments

We thank Drs. R. B. Gennis for the plasmid pJRHisA(cyoABCD), A. Dancis for help with performing Fe uptake kinetics, and M. Goulian for providing *E. coli* strains, phage, and plasmids.

Author Contributions

Conceptualization: Crysten E. Blaby-Haas, Fevzi Daldal.

Data curation: Fevzi Daldal.

Formal analysis: Bahia Khalfaoui-Hassani, Crysten E. Blaby-Haas, Andreia Verissimo.

Funding acquisition: Crysten E. Blaby-Haas, Fevzi Daldal.

Investigation: Bahia Khalfaoui-Hassani, Fevzi Daldal.

Methodology: Andreia Verissimo.

Visualization: Crysten E. Blaby-Haas.

Writing – original draft: Bahia Khalfaoui-Hassani, Crysten E. Blaby-Haas.

Writing – review & editing: Bahia Khalfaoui-Hassani, Crysten E. Blaby-Haas, Andreia Verissimo, Fevzi Daldal.

References

1. Ekici S, Pawlik G, Lohmeyer E, Koch HG, Daldal F (2012) Biogenesis of cbb(3)-type cytochrome c oxidase in Rhodobacter capsulatus. Biochim Biophys Acta 1817:898–910. https://doi.org/10.1016/j.bbabio.2011.10.011 PMID: 22079199
2. Andrei A, Ozturk Y, Khalfaoui-Hassani B, Rauch J, Marckmann D, Trasnea PI, Daldal F, Koch HG (2020) Cu Homeostasis in Bacteria: The Ins and Outs. Membranes (Basel) 10. https://doi.org/10.3390/membranes10090242 PMID: 32962054
3. Friedrich T, Wohlwend D, Borisov VB (2022) Recent Advances in Structural Studies of Cytochrome bd and Its Potential Application as a Drug Target. Int J Mol Sci 23. https://doi.org/10.3390/ijms23063166 PMID: 35328590
4. Garcia-Horsman JA, Barquera B, Rumbley J, Ma J, Gennis RB (1994) The superfamily of heme-copper respiratory oxidases. J Bacteriol 176:5587–600. https://doi.org/10.1128/jb.176.18.5587-5600.1994 PMID: 8083153
5. Pereira MM, Teixeira M (2004) Proton pathways, ligand binding and dynamics of the catalytic site in haem-copper oxygen reductases: a comparison between the three families. Biochim Biophys Acta 1655:340–6. https://doi.org/10.1016/j.bbabio.2003.06.003 PMID: 15100049
6. Borisov VB, Siletsky SA (2019) Features of Organization and Mechanism of Catalysis of Two Families of Terminal Oxidases: Heme-Copper and bd-Type. Biochemistry (Mosc) 84:1390–1402. https://doi.org/10.1134/S0006297919110130 PMID: 31760925
7. Tsukihara T, Aoyama H, Yamashita E, Tomizaki T, Yamaguchi H, Shinzawa-Itoh K, Nakashima R, Yaono R, Yoshikawa S (1996) The whole structure of the 13-subunit oxidized cytochrome c oxidase at 2.8 A. Science 272:1136–44. https://doi.org/10.1126/science.272.5265.1136 PMID: 8638158
8. Ostermeier C, Harrenga A, Ermler U, Michel H (1997) Structure at 2.7 A resolution of the Paracoccus denitrificans two-subunit cytochrome c oxidase complexed with an antibody FV fragment. Proc Natl Acad Sci U S A 94:10547–53. https://doi.org/10.1073/pnas.94.20.10547 PMID: 9380672
9. Zong S, Wu M, Gu J, Liu T, Guo R, Yang M (2018) Structure of the intact 14-subunit human cytochrome c oxidase. Cell Res 28:1026–1034. https://doi.org/10.1038/s41422-018-0071-1 PMID: 30030519
10. Buschmann S, Warkentin E, Xie H, Langer JD, Ermler U, Michel H (2010) The structure of cbb3 cytochrome oxidase provides insights into proton pumping. Science 329:327–30. https://doi.org/10.1126/science.1187303 PMID: 20576851
11. Khalfaoui-Hassani B, Verissimo AF, Koch HG, Daldal F (2016). Uncovering the Transmembrane Metal Binding Site of the Novel Bacterial Major Facilitator Superfamily-Type Copper Importer CcoA. mBio 7: e01981–15. https://doi.org/10.1128/mBio.01981-15 PMID: 26787831
12. Khalfaoui-Hassani B, Verissimo AF, Shroff NP, Ekici S, Trasnea P-I, Utz M, Koch H-G, Daldal F (2016) Biogenesis of Cytochrome c complexes: From Insertion of redox cofactors to Assembly of different subunits. Springer, Dordrecht, Netherlands.
13. Abramson J, Riistama S, Larsson G, Jasaitis A, Svensson-Ek M, Laakkonen L, Puustinen A, Iwata S, Wikstrom M (2000) The structure of the ubiquinol oxidase from Escherichia coli and its ubiquinone binding site. Nat Struct Biol 7:910–7. https://doi.org/10.1038/82824 PMID: 11017202

14. Chepuri V, Lemieux L, Au DC, Gennis RB (1990) The sequence of the cyo operon indicates substantial structural similarities between the cytochrome o ubiquinol oxidase of Escherichia coli and the aa3-type family of cytochrome c oxidases. J Biol Chem 265:11185–92. PMID: 2162835

15. Sousa FL, Alves RJ, Ribeiro MA, Pereira-Leal JB, Teixeira M, Pereira MM (2012) The superfamily of heme-copper oxygen reductases: types and evolutionary considerations. Biochim Biophys Acta 1817:629–37. https://doi.org/10.1016/j.bbabio.2011.09.020 PMID: 22001780

16. Murali R, Hemp J, Gennis RB (2022) Evolution of quinol oxidation within the heme-copper oxidoreductase superfamily. Biochim Biophys Acta Bioenerg 1863:148907.

17. Borisov VB, Gennis RB, Hemp J, Verkhovsky MI (2011) The cytochrome bd respiratory oxygen reductases. Biochim Biophys Acta 1807:1398–413. https://doi.org/10.1016/j.bbabio.2011.06.016 PMID: 21756872

18. Safarian S, Rajendran C, Muller H, Preu J, Langer JD, Ovchinnikov S, Hirose T, Kusumoto T, Sakamoto J, Michel H (2016) Structure of a bd oxidase indicates similar mechanisms for membrane-integrated oxygen reductases. Science 352:583–6. https://doi.org/10.1126/science.aaf2477 PMID: 27126043

19. Sanders C, Turkarslan S, Lee DW, Daldal F (2010) Cytochrome c biogenesis: the Ccm system. Trends Microbiol 18:266–74. https://doi.org/10.1016/j.tim.2010.03.006 PMID: 20382024

20. Koch H-G, Schneider D (2016) Assembly of transmembrane b-type cytochromes amnd cytochrome complexes, p 555–584. *In* Cramer WA, Kallas T (ed), Cytochrome complexes: evolution, structures, energy transduction and signaling. Springer.

21. Smith D, Gray J, Mitchell L, Antholine WE, Hosler JP (2005) Assembly of cytochrome-c oxidase in the absence of assembly protein Surf1p leads to loss of the active site heme. J Biol Chem 280:17652–6. https://doi.org/10.1074/jbc.C500061200 PMID: 15764605

22. Bundschuh FA, Hoffmeier K, Ludwig B (2008) Two variants of the assembly factor Surf1 target specific terminal oxidases in Paracoccus denitrificans. Biochim Biophys Acta 1777:1336–43. https://doi.org/10.1016/j.bbabio.2008.05.448 PMID: 18582433

23. Bundschuh FA, Hannappel A, Anderka O, Ludwig B (2009) Surf1, associated with Leigh syndrome in humans, is a heme-binding protein in bacterial oxidase biogenesis. J Biol Chem 284:25735–41. https://doi.org/10.1074/jbc.M109.040295 PMID: 19625251

24. Davoudi CF, Ramp P, Baumgart M, Bott M (2019) Identification of Surf1 as an assembly factor of the cytochrome bc(1)-aa(3) supercomplex of Actinobacteria. Biochim Biophys Acta Bioenerg 1860:148033. https://doi.org/10.1016/j.bbabio.2019.06.005 PMID: 31226315

25. Werner C, Richter OM, Ludwig B (2010) A novel heme a insertion factor gene cotranscribes with the Thermus thermophilus cytochrome ba3 oxidase locus. J Bacteriol 192:4712–9. https://doi.org/10.1128/JB.00548-10 PMID: 20622059

26. Koch HG, Winterstein C, Saribas AS, Alben JO, Daldal F (2000) Roles of the ccoGHIS gene products in the biogenesis of the cbb(3)-type cytochrome c oxidase. J Mol Biol 297:49–65. https://doi.org/10.1006/jmbi.2000.3555 PMID: 10704306

27. Kulajta C, Thumfart JO, Haid S, Daldal F, Koch HG (2006) Multi-step assembly pathway of the cbb3-type cytochrome c oxidase complex. J Mol Biol 355:989–1004. https://doi.org/10.1016/j.jmb.2005.11.039 PMID: 16343536

28. Hoeser J, Hong S, Gehmann G, Gennis RB, Friedrich T (2014) Subunit CydX of Escherichia coli cytochrome bd ubiquinol oxidase is essential for assembly and stability of the di-heme active site. FEBS Lett 588:1537–41. https://doi.org/10.1016/j.febslet.2014.03.036 PMID: 24681096

29. Chen H, Luo Q, Yin J, Gao T, Gao H (2015) Evidence for the requirement of CydX in function but not assembly of the cytochrome bd oxidase in Shewanella oneidensis. Biochim Biophys Acta 1850:318–28. https://doi.org/10.1016/j.bbagen.2014.10.005 PMID: 25316290

30. Ekim Kocabey A, Kost L, Gehlhar M, Rodel G, Gey U (2019) Mitochondrial Sco proteins are involved in oxidative stress defense. Redox Biol 21:101079. https://doi.org/10.1016/j.redox.2018.101079 PMID: 30593977

31. Lohmeyer E, Schroder S, Pawlik G, Trasnea PI, Peters A, Daldal F, Koch HG (2012) The ScoI homologue SenC is a copper binding protein that interacts directly with the cbb(3)-type cytochrome oxidase in Rhodobacter capsulatus. Biochim Biophys Acta 1817:2005–15.

32. Trasnea PI, Utz M, Khalfaoui-Hassani B, Lagies S, Daldal F, Koch HG (2016) Cooperation between two periplasmic copper chaperones is required for full activity of the cbb3 -type cytochrome c oxidase and copper homeostasis in Rhodobacter capsulatus. Mol Microbiol 100:345–61. https://doi.org/10.1111/mmi.13321 PMID: 26718481

33. Trasnea PI, Andrei A, Marckmann D, Utz M, Khalfaoui-Hassani B, Selamoglu N, Daldal F, Koch HG (2018) A Copper Relay System Involving Two Periplasmic Chaperones Drives cbb(3)-Type

Cytochrome c Oxidase Biogenesis in Rhodobacter capsulatus. ACS Chem Biol 13:1388–1397. https://doi.org/10.1021/acschembio.8b00293 PMID: 29613755

34. Canonica F, Klose D, Ledermann R, Sauer MM, Abicht HK, Quade N, Gossert AD, Chesnov S, Fischer HM, Jeschke G, Hennecke H, Glockshuber R (2019) Structural basis and mechanism for metallochaperone-assisted assembly of the Cu(A) center in cytochrome oxidase. Sci Adv 5:eaaw8478. https://doi.org/10.1126/sciadv.aaw8478 PMID: 31392273

35. Banci L, Bertini I, Ciofi-Baffoni S, Katsari E, Katsaros N, Kubicek K, Mangani S (2005) A copper(I) protein possibly involved in the assembly of CuA center of bacterial cytochrome c oxidase. Proc Natl Acad Sci U S A 102:3994–9. https://doi.org/10.1073/pnas.0406150102 PMID: 15753304

36. Hiser L, Di Valentin M, Hamer AG, Hosler JP (2000) Cox11p is required for stable formation of the Cu (B) and magnesium centers of cytochrome c oxidase. J Biol Chem 275:619–23. https://doi.org/10.1074/jbc.275.1.619 PMID: 10617659

37. Carr HS, George GN, Winge DR (2002) Yeast Cox11, a protein essential for cytochrome c oxidase assembly, is a Cu(I)-binding protein. J Biol Chem 277:31237–42. https://doi.org/10.1074/jbc.M204854200 PMID: 12063264

38. Thompson AK, Gray J, Liu A, Hosler JP (2012) The roles of Rhodobacter sphaeroides copper chaperones PCu(A)C and Sco (PrrC) in the assembly of the copper centers of the aa(3)-type and the cbb(3)-type cytochrome c oxidases. Biochim Biophys Acta 1817:955–64. https://doi.org/10.1016/j.bbabio.2012.01.003 PMID: 22248670

39. Radin I, Kost L, Gey U, Steinebrunner I, Rodel G (2021) The mitochondrial copper chaperone COX11 has an additional role in cellular redox homeostasis. PLoS One 16:e0261465. https://doi.org/10.1371/journal.pone.0261465 PMID: 34919594

40. Horng YC, Cobine PA, Maxfield AB, Carr HS, Winge DR (2004) Specific copper transfer from the Cox17 metallochaperone to both Sco1 and Cox11 in the assembly of yeast cytochrome C oxidase. J Biol Chem 279:35334–40. https://doi.org/10.1074/jbc.M404747200 PMID: 15199057

41. Banci L, Bertini I, Ciofi-Baffoni S, Hadjiloi T, Martinelli M, Palumaa P (2008) Mitochondrial copper(I) transfer from Cox17 to Sco1 is coupled to electron transfer. Proc Natl Acad Sci U S A 105:6803–8. https://doi.org/10.1073/pnas.0800019105 PMID: 18458339

42. Shi H, Jiang Y, Yang Y, Peng Y, Li C (2021) Copper metabolism in Saccharomyces cerevisiae: an update. Biometals 34:3–14. https://doi.org/10.1007/s10534-020-00264-y PMID: 33128172

43. Marckmann D, Trasnea PI, Schimpf J, Winterstein C, Andrei A, Schmollinger S, Blaby-Haas CE, Friedrich T, Daldal F, Koch HG (2019) The cbb(3)-type cytochrome oxidase assembly factor CcoG is a widely distributed cupric reductase. Proc Natl Acad Sci U S A 116:21166–21175. https://doi.org/10.1073/pnas.1913803116 PMID: 31570589

44. Gonzalez-Guerrero M, Raimunda D, Cheng X, Arguello JM (2010) Distinct functional roles of homologous Cu+ efflux ATPases in Pseudomonas aeruginosa. Mol Microbiol 78:1246–58. https://doi.org/10.1111/j.1365-2958.2010.07402.x PMID: 21091508

45. Hassani BK, Astier C, Nitschke W, Ouchane S (2010) CtpA, a copper-translocating P-type ATPase involved in the biogenesis of multiple copper-requiring enzymes. J Biol Chem 285:19330–7. https://doi.org/10.1074/jbc.M110.116020 PMID: 20363758

46. Ekici S, Yang H, Koch HG, Daldal F (2012) Novel transporter required for biogenesis of cbb3-type cytochrome c oxidase in Rhodobacter capsulatus. mBio 3. https://doi.org/10.1128/mBio.00293-11 PMID: 22294680

47. Ekici S, Turkarslan S, Pawlik G, Dancis A, Baliga NS, Koch HG, Daldal F (2014) Intracytoplasmic copper homeostasis controls cytochrome c oxidase production. mBio 5:e01055–13. https://doi.org/10.1128/mBio.01055-13 PMID: 24425735

48. Zhang Y, Blaby-Haas CE, Steimle S, Verissimo AF, Garcia-Angulo VA, Koch HG, Daldal F, Khalfaoui-Hassani B (2019) Cu Transport by the Extended Family of CcoA-like Transporters (CalT) in Proteobacteria. Sci Rep 9:1208. https://doi.org/10.1038/s41598-018-37988-4 PMID: 30718766

49. Khalfaoui-Hassani B, Wu HJ, Blaby-Haas CE, Zhang Y, Sandri F, Verissimo AF, Koch HG, Daldal F (2018) Widespread Distribution and Functional Specificity of the Copper Importer CcoA: Distinct Cu Uptake Routes for Bacterial Cytochrome c Oxidases. Mbio 9. https://doi.org/10.1128/mBio.00065-18 PMID: 29487231

50. Abicht HK, Scharer MA, Quade N, Ledermann R, Mohorko E, Capitani G, Hennecke H, Glockshuber R (2014) How periplasmic thioredoxin TlpA reduces bacterial copper chaperone ScoI and cytochrome oxidase subunit II (CoxB) prior to metallation. J Biol Chem 289:32431–44. https://doi.org/10.1074/jbc.M114.607127 PMID: 25274631

51. Canonica F, Hennecke H, Glockshuber R (2019) Biochemical pathway for the biosynthesis of the Cu(A) center in bacterial cytochrome c oxidase. FEBS Lett 593:2977–2989. https://doi.org/10.1002/1873-3468.13587 PMID: 31449676

52. Quistgaard EM, Low C, Guettou F, Nordlund P (2016) Understanding transport by the major facilitator superfamily (MFS): structures pave the way. Nat Rev Mol Cell Biol 17:123–32. https://doi.org/10.1038/nrm.2015.25 PMID: 26758938

53. Wang SC, Davejan P, Hendargo KJ, Javadi-Razaz I, Chou A, Yee DC, Ghazi F, Lam KJK, Conn AM, Madrigal A, Medrano-Soto A, Saier MH Jr (2020) Expansion of the Major Facilitator Superfamily (MFS) to include novel transporters as well as transmembrane-acting enzymes. Biochim Biophys Acta Biomembr 1862:183277. https://doi.org/10.1016/j.bbamem.2020.183277 PMID: 32205149

54. Baba T, Ara T, Hasegawa M, Takai Y, Okumura Y, Baba M, Datsenko KA, Tomita M, Wanner BL, Mori H (2006) Construction of Escherichia coli K-12 in-frame, single-gene knockout mutants: the Keio collection. Mol Syst Biol 2:2006 0008. https://doi.org/10.1038/msb4100050 PMID: 16738554

55. Libby EA, Ekici S, Goulian M (2010) Imaging OmpR binding to native chromosomal loci in Escherichia coli. J Bacteriol 192:4045–53. https://doi.org/10.1128/JB.00344-10 PMID: 20511496

56. Zallot R, Oberg N, Gerlt JA (2019) The EFI Web Resource for Genomic Enzymology Tools: Leveraging Protein, Genome, and Metagenome Databases to Discover Novel Enzymes and Metabolic Pathways. Biochemistry 58:4169–4182. https://doi.org/10.1021/acs.biochem.9b00735 PMID: 31553576

57. Shannon P, Markiel A, Ozier O, Baliga NS, Wang JT, Ramage D, Amin N, Schwikowski B, Ideker T (2003) Cytoscape: a software environment for integrated models of biomolecular interaction networks. Genome Res 13:2498–504. https://doi.org/10.1101/gr.1239303 PMID: 14597658

58. Miller MA, Pfeiffer W, Schwartz T (2010) Creating the CIPRES Science Gateway for inference of large phylogenetic trees. Proceedings of the Gateway Computing Environments Workshop:1–8.

59. Katoh K, Standley DM (2013) MAFFT multiple sequence alignment software version 7: improvements in performance and usability. Mol Biol Evol 30:772–80. https://doi.org/10.1093/molbev/mst010 PMID: 23329690

60. Trifinopoulos J, Nguyen LT, von Haeseler A, Minh BQ (2016) W-IQ-TREE: a fast online phylogenetic tool for maximum likelihood analysis. Nucleic Acids Res 44:W232–5. https://doi.org/10.1093/nar/gkw256 PMID: 27084950

61. Letunic I, Bork P (2021) Interactive Tree Of Life (iTOL) v5: an online tool for phylogenetic tree display and annotation. Nucleic Acids Res 49:W293–W296. https://doi.org/10.1093/nar/gkab301 PMID: 33885785

62. Rubino JT, Franz KJ (2012) Coordination chemistry of copper proteins: how nature handles a toxic cargo for essential function. J Inorg Biochem 107:129–43. https://doi.org/10.1016/j.jinorgbio.2011.11.024 PMID: 22204943

63. Anraku Y, Gennis RB (1987) The Aerobic Respiratory-Chain of Escherichia-Coli. Trends in Biochemical Sciences 12:262–266.

64. Puustinen A, Finel M, Haltia T, Gennis RB, Wikstrom M (1991) Properties of the two terminal oxidases of Escherichia coli. Biochemistry 30:3936–42. https://doi.org/10.1021/bi00230a019 PMID: 1850294

65. Dassa J, Fsihi H, Marck C, Dion M, Kieffer-Bontemps M, Boquet PL (1991) A new oxygen-regulated operon in Escherichia coli comprises the genes for a putative third cytochrome oxidase and for pH 2.5 acid phosphatase (appA). Mol Gen Genet 229:341–52. https://doi.org/10.1007/BF00267454 PMID: 1658595

66. Borisov VB, Murali R, Verkhovskaya ML, Bloch DA, Han H, Gennis RB, Verkhovsky MI (2011) Aerobic respiratory chain of Escherichia coli is not allowed to work in fully uncoupled mode. Proc Natl Acad Sci U S A 108:17320–4. https://doi.org/10.1073/pnas.1108217108 PMID: 21987791

67. Sturr MG, Krulwich TA, Hicks DB (1996) Purification of a cytochrome bd terminal oxidase encoded by the Escherichia coli app locus from a delta cyo delta cyd strain complemented by genes from Bacillus firmus OF4. J Bacteriol 178:1742–9. https://doi.org/10.1128/jb.178.6.1742-1749.1996 PMID: 8626304

68. Rumbley JN, Furlong Nickels E, Gennis RB (1997) One-step purification of histidine-tagged cytochrome bo3 from Escherichia coli and demonstration that associated quinone is not required for the structural integrity of the oxidase. Biochim Biophys Acta 1340:131–42. https://doi.org/10.1016/s0167-4838(97)00036-8 PMID: 9217023

69. Puustinen A, Wikstrom M (1991) The heme groups of cytochrome o from Escherichia coli. Proc Natl Acad Sci U S A 88:6122–6. https://doi.org/10.1073/pnas.88.14.6122 PMID: 2068092

70. Laranjeira-Silva MF, Wang W, Samuel TK, Maeda FY, Michailowsky V, Hamza I, Liu Z, Andrews NW (2018) A MFS-like plasma membrane transporter required for Leishmania virulence protects the parasites from iron toxicity. PLoS Pathog 14:e1007140. https://doi.org/10.1371/journal.ppat.1007140 PMID: 29906288

71. Furrer JL, Sanders DN, Hook-Barnard IG, McIntosh MA (2002) Export of the siderophore enterobactin in Escherichia coli: involvement of a 43 kDa membrane exporter. Mol Microbiol 44:1225–34. https://doi.org/10.1046/j.1365-2958.2002.02885.x PMID: 12068807

72. Miethke M, Schmidt S, Marahiel MA (2008) The major facilitator superfamily-type transporter YmfE and the multidrug-efflux activator Mta mediate bacillibactin secretion in Bacillus subtilis. J Bacteriol 190:5143–52. https://doi.org/10.1128/JB.00464-08 PMID: 18502870

73. Rodionov DA, Vitreschak AG, Mironov AA, Gelfand MS (2002) Comparative genomics of thiamin biosynthesis in procaryotes. New genes and regulatory mechanisms. J Biol Chem 277:48949–59. https://doi.org/10.1074/jbc.M208965200 PMID: 12376536

74. Johansson L, Liden G (2006) Transcriptome analysis of a shikimic acid producing strain of Escherichia coli W3110 grown under carbon- and phosphate-limited conditions. J Biotechnol 126:528–45. https://doi.org/10.1016/j.jbiotec.2006.05.007 PMID: 16828913

75. Wang C, Yang L, Shah AA, Choi ES, Kim SW (2015) Dynamic interplay of multidrug transporters with TolC for isoprenol tolerance in Escherichia coli. Sci Rep 5:16505. https://doi.org/10.1038/srep16505 PMID: 26563610

76. Fan Y, Cross PJ, Jameson GB, Parker EJ (2018) Exploring modular allostery via interchangeable regulatory domains. Proc Natl Acad Sci U S A 115:3006–3011. https://doi.org/10.1073/pnas.1717621115 PMID: 29507215

77. Koita K, Rao CV (2012) Identification and analysis of the putative pentose sugar efflux transporters in Escherichia coli. PLoS One 7:e43700. https://doi.org/10.1371/journal.pone.0043700 PMID: 22952739

78. Staub JM, Brand L, Tran M, Kong Y, Rogers SG (2012) Bacterial glyphosate resistance conferred by overexpression of an E. coli membrane efflux transporter. J Ind Microbiol Biotechnol 39:641–7. https://doi.org/10.1007/s10295-011-1057-x PMID: 22089966

79. Blaise M, Becker HD, Lapointe J, Cambillau C, Giege R, Kern D (2005) Glu-Q-tRNA(Asp) synthetase coded by the yadB gene, a new paralog of aminoacyl-tRNA synthetase that glutamylates tRNA(Asp) anticodon. Biochimie 87:847–61. https://doi.org/10.1016/j.biochi.2005.03.007 PMID: 16164993

80. Babu M, Bundalovic-Torma C, Calmettes C, Phanse S, Zhang Q, Jiang Y, Minic Z, Kim S, Mehla J, Gagarinova A, Rodionova I, Kumar A, Guo H, Kagan O, Pogoutse O, Aoki H, Deineko V, Caufield JH, Holtzapple E, Zhang Z, Vastermark A, Pandya Y, Lai CC, El Bakkouri M, Hooda Y, Shah M, Burnside D, Hooshyar M, Vlasblom J, Rajagopala SV, Golshani A, Wuchty S, J FG, Saier M, Uetz P, T FM, Parkinson J, Emili A (2018) Global landscape of cell envelope protein complexes in Escherichia coli. Nat Biotechnol 36:103–112. https://doi.org/10.1038/nbt.4024 PMID: 29176613

81. Coulton JW, Mason P, DuBow MS (1983) Molecular cloning of the ferrichrome-iron receptor of Escherichia coli K-12. J Bacteriol 156:1315–21. https://doi.org/10.1128/jb.156.3.1315-1321.1983 PMID: 6315686

82. Herrmann KM (1995) The Shikimate Pathway: Early Steps in the Biosynthesis of Aromatic Compounds. Plant Cell 7:907–919. https://doi.org/10.1105/tpc.7.7.907 PMID: 12242393

83. Mir R, Jallu S, Singh TP (2015) The shikimate pathway: review of amino acid sequence, function and three-dimensional structures of the enzymes. Crit Rev Microbiol 41:172–89. https://doi.org/10.3109/1040841X.2013.813901 PMID: 23919299

84. Baasov T, Knowles JR (1989) Is the first enzyme of the shikimate pathway, 3-deoxy-D-arabino-heptulosonate-7-phosphate synthase (tyrosine sensitive), a copper metalloenzyme? J Bacteriol 171:6155–60. https://doi.org/10.1128/jb.171.11.6155-6160.1989 PMID: 2572582

85. Imlay JA (2014) The mismetallation of enzymes during oxidative stress. J Biol Chem 289:28121–8. https://doi.org/10.1074/jbc.R114.588814 PMID: 25160623